

Elevated Anthropogenic Contributions to Trace Elements in Marine Aerosols Compared to Coastal Qingdao in Eastern China

Yuxuan Qi^{1,2}, Wenshuai Li^{1,2,3,4}, Wen Qu⁵, Haizhou Zhang⁵, Wenqing Zhu^{1,2}, Jinhui Shi^{3,4}, Daizhou Zhang⁶, Yanjing Zhang^{1,2}, Lifang Sheng^{1,2}, Wencai Wang^{1,2}, Yunhui Zhao^{1,2}, Yuanyuan Ma^{1,2}, Danyang Ren^{1,2}, Guanru Wu^{1,2}, Xinfeng Wang⁷, Xiaohong Yao^{3,4}, Yang Zhou^{1,2*}

¹State Key Laboratory of Physical Oceanography, Ocean University of China, Qingdao, 266100, China

²College of Oceanic and Atmospheric Sciences, Ocean University of China, Qingdao, 266100, China

³Key Laboratory of Marine Environment and Ecology, Ministry of Education, Ocean University of China, Qingdao, 266100, China

10 ⁴Laboratory for Marine Ecology and Environmental Science, Qingdao National Laboratory for Marine Science and Technology, Qingdao, 266237, China

⁵North Sea Bureau of Ministry of Natural Resources of the People's Republic of China, Qingdao, 266061, China

⁶Faculty of Environmental and Symbiotic Sciences, Prefectural University of Kumamoto, 862-8502, Japan

⁷Environment Research Institute, Shandong University, Qingdao, 266237, China

15 *Correspondence to:* Yang Zhou (yangzhou@ouc.edu.cn)

Abstract. Long-range transport of trace elements (TEs) by aerosols plays a critical role in modulating marine biogeochemistry; yet, their source contributions and spatial variability across land-sea gradients remain poorly constrained. Here, we investigate TEs (e.g., Fe, Mn, Cr, V, Ni, Cu, Zn, As, Pb, Cd) in PM_{2.5} aerosols collected from the coastal city of Qingdao (eastern China) and adjacent offshore regions (Bohai Sea and Yellow Sea) during spring and summer 2018, to quantify terrestrial vs. marine source contributions and unravel key drivers of their spatial patterns. All TEs exhibited higher concentrations in Qingdao than in offshore marine areas in spring, whereas Zn, Pb, As, and Cd (52.5–78.8% from coal combustion over the marine areas) reversed to higher concentrations in offshore marine areas than in Qingdao in summer, indicating intensified anthropogenic impact on the marine atmosphere. For traditional crustal TEs (Fe, Mn, Cr), terrestrial dust dominated in spring Qingdao (e.g., Fe: 62.3%, 148.6 ng m⁻³), but dust contributions declined sharply in spring offshore marine areas (Fe: 16.8%, 52.3 ng m⁻³). Instead, coal combustion emerged as the dominant source in summer offshore marine aerosols (Fe: 43.2%, 82.8 ng m⁻³), exceeding its contribution to Qingdao (Fe: 14.45%, 45.46 ng m⁻³). Ship emissions dominated sources of Ni and V (V: 81.2% in spring, 90.5% in summer) and contributed significantly to Fe, Mn, and Cr, particularly in summer offshore aerosols (e.g., Fe: 27.4%, 52.5 ng m⁻³). Spring offshore marine aerosols showed elevated sea salt contributions to Fe, Mn, Zn, Cd, and Pb (18.5–33.6%), indicating extensive multi-source mixing (dust, sea salt, and anthropogenic sources); the biogeochemical implications of this mixing for element reactivity warrant further investigation. These findings highlight the dominant role of anthropogenic emissions (coal combustion and shipping) in shaping the TE composition of offshore aerosols over the Bohai and Yellow Seas. This work advances our understanding of land-sea interactions in atmospheric TE cycling and offers critical constraints for regional air quality and climate models.

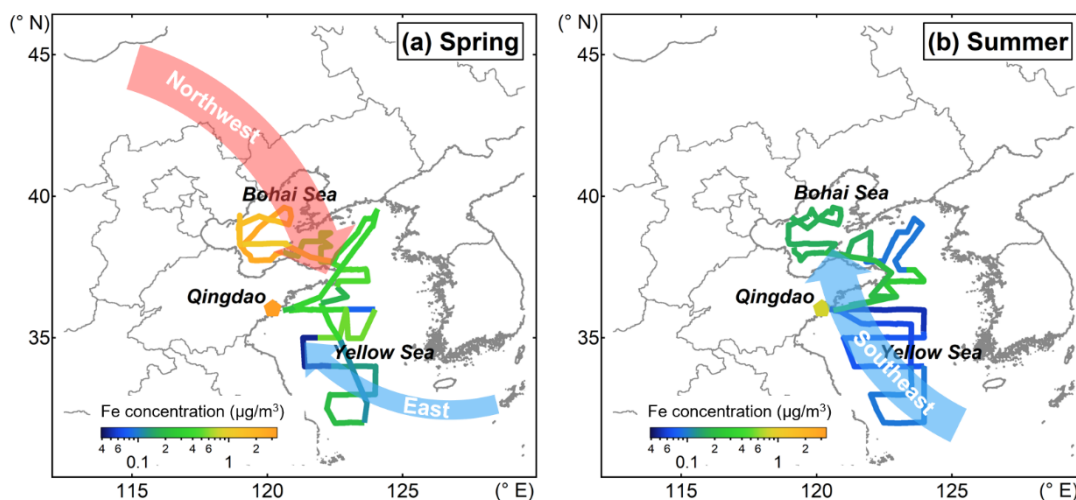
1 Introduction

35 Atmospheric aerosols can significantly impact the local environment and global climate change through modifying the solar radiation balance in the atmosphere (Huang et al., 2014; Ramanathan et al., 2007) and supplying nutrients to ecosystems (Chooari et al., 2014). Anthropogenic activities release a profusion of pollutants that can engage in intricate physicochemical processes, resulting in the formation of atmospheric fine particulate matter ($D_p \leq 2.5 \mu\text{m}$, $\text{PM}_{2.5}$). Distinct from large-diameter particles, these primary or secondary $\text{PM}_{2.5}$ usually possess long lifetimes, which are capable of undergoing long-range
40 transport in the atmosphere and depositing into remote oceans. This process introduces substantial anthropogenic pollutants, thereby impacting ocean ecosystems (Mahowald, 2011; Xu et al., 2021).

Despite trace elements constituting only a minor fraction of the $\text{PM}_{2.5}$ mass, their significant post-deposition impacts on downwind marine ecosystems have attracted considerable attention (Li et al., 2015; Morel and Price, 2003; Zhang et al., 2018). Some trace elements deposited in the open oceans, such as Mn, Fe, Ni, Cu, Zn, and Cd, have biological roles, generally as
45 cofactors or part of cofactors of enzymes or as structural elements in proteins (Morel and Price, 2003). These elements can markedly influence the growth of phytoplankton taxa and the biological community structure of marine organisms, thereby affecting carbon sequestration and marine primary production (Boyd et al., 2000; Falkowski et al., 1998; Mann et al., 2002; Martin, 1990; Morel and Price, 2003; Yoon et al., 2018; Tang et al., 2021). The total fraction of trace elements cannot be fully utilized by marine biota. In most cases, only the soluble fractions are more likely to be bioavailable (Shi et al., 2012), and the
50 solubility is closely associated with their sources (Baker et al., 2006; Sholkovitz et al., 2012). For instance, while mineral dust is the principal source of Fe, numerous studies have demonstrated that Fe emitted from anthropogenic sources has a higher solubility (López-García et al., 2017; Sholkovitz et al., 2012; Sun et al., 2024). Model results also suggest that the combustion-derived Fe tended to account for over 20% of the Fe deposition near the Asian continent, and the efficiency of pyrogenic Fe in enhancing marine productivity exceeds that of lithogenic sources (Ito et al., 2021; Luo et al., 2008). Fe from the combustion
55 source is typically present in finer particles (Buck et al., 2010; Ito and Feng, 2011).

The Bohai Sea (BS) and Yellow Sea (YS) are on the crucial transport pathway for aerosols originating from the heavily polluted East Asia area to the Northwest Pacific within the westerly belt. Qingdao (QD) is a coastal city adjacent to YS (Fig.1). Aerosol trace elements over the BS and YS likely exhibit distinct characteristics compared to those in coastal cities, necessitating synchronized land-sea observations to investigate these characteristics. However, as previously noted, the current knowledge
60 regarding the source apportionment of trace elements in marine aerosols remains limited (Hilario et al., 2020). Prior field cruise investigations have focused on the characteristics of total suspended particulates (TSP) and PM_{10} ($D_p \leq 10 \mu\text{m}$) (Hsu et al., 2010; Li et al., 2025; Peng et al., 2025; Qiu, 2015; Shi et al., 2013; Wang et al., 2013; Yang et al., 2020). In contrast, trace elements in $\text{PM}_{2.5}$ have been scarcely explored. It has been revealed that trace elements in fine particles exhibit distinct potential environmental impacts with coarse particles (Li et al., 2018; Hsieh et al., 2022; Sakata et al., 2022; Zhang et al., 2022),
65 highlighting the importance of targeting $\text{PM}_{2.5}$.

70 Atmospheric processes during long-range transport from the continent to ocean can alter the physicochemical properties of aerosols, thereby influencing the bioavailability of nutrients in the particles upon deposition (Schroth et al., 2009; Sholkovitz et al., 2012; Wang et al., 2022; Wang et al., 2021; Luo et al., 2020; Xu et al., 2023; Zhang et al., 2024). Accurately identifying and apportioning the sources of fine particles and their trace elements, particularly their differences across land-to-sea gradients, is crucial for quantifying this biogeochemical impact, especially given the differences observed across land-to-sea gradients. This study focuses on the characteristics and source apportionment of elements in $PM_{2.5}$, based on simultaneous observations in Qingdao and during BS and YS research cruises in the spring and summer of 2018 (Fig.1). The major purpose is to provide a more comprehensive understanding of the distribution and sources of trace elements in fine particles from coastal to marginal sea areas in eastern China.



75

Figure 1: Schematic diagram of regional maps with dominant air mass transport pathways (arrows). The solid lines indicate cruise tracks for (a) springtime and (b) summertime cruises over BS and YS during 2018 and the star indicates the location of Qingdao, with the color-filled indicating Fe concentration.

2 Methodology

80 2.1 Sample collection

PM_{2.5} samples were collected to measure fine particle components over the BS, YS, and Qingdao during the spring and summer of 2018. In the cruise missions, the samples were collected over the BS and YS from 28 March to 17 April and from 24 July to 10 August 2018. These areas are located in the downwind areas of the Asian dust source regions and northern China city groups being significantly influenced by dust and anthropogenic pollution (Fig.1). A total of 18 and 9 samples were collected in spring and summer over the marine areas, respectively. Specifically, these comprised 3 samples from the BS and 15 from the YS in spring, and 2 from the BS and 7 from the YS in summer. Sampling durations varied from several hours to 28 hours in spring and from 18 to approximately 40 hours in summer to accumulate sufficient particle mass. During the collection of

85

marine aerosols, samples were exclusively collected while the ship was underway and the relative wind direction ranged between -60° and $+60^{\circ}$ (with 0° representing the bow) to avoid contamination from the vessel's own exhaust emissions.

90 The samples in Qingdao were collected in the same period as the cruise missions. The sampling site was located at the Baguanshan Atmospheric Research Observatory (BARO, 36.03° N, 120.20° E; 74 m above sea level) in the Shinan District Qingdao (Fig.1), with an approximately 600 m straight-line distance from the coastline (Li et al., 2024; Yang et al., 2024). In Qingdao, 37 and 25 samples were collected during non-rainy periods in spring and summer, respectively. At the coastal site, a day/night sampling strategy was primarily employed, and a few summer samples were collected over about 23-hour periods.

95 High-volume particle samplers (Tisch Environmental, Inc., USA and Qingdao Jinshida Electronic Technology Co., Ltd., China) were applied to collect the particles onto Whatman[®] 41# filters (Whatman Limited, Maidstone, UK) for trace element analysis, and onto PALL[®] quartz filters (Pall Gelman, Inc., USA) for analysis of water-soluble ions, organic carbon (OC), and elemental carbon (EC). The 41# filters were washed with diluted acid prior to sampling following Chance et al. (2015) to remove background trace elements. Quartz filters were pre-baked at 450° C for 6 hours before the sample collection to eliminate

100 background organic contaminants. For quality assurance and control, blank filters were collected and processed, with detailed results and their impact assessment provided in Text S1a and Table S1. All samples were sealed in plastic bags and stored at -20° C until subsequent analysis.

2.2 Chemical analysis

Trace elements: An 8.0 cm^2 section of both the sample and blank filters was digested with an acid mixture (2.0 mL of 69% HNO₃ and 0.5 mL of 40% HF) in closed Teflon vessels and heated at 180° C for 48 h. After cooling to room temperature, the solutions were evaporated to near dryness at 180° C using an electric heating plate (Text S1a). Then, the residue was diluted to 50 mL with 2% HNO₃ and stored at $\sim 4^{\circ}$ C until analysis.

105

The concentrations of elements in the extracts were measured using an inductively coupled plasma-mass spectrometry (ICP-MS, iCAP Qc, Thermo Fisher Scientific, Germany) with internal standards of Rh, Sc, and Th to eliminate matrix interference.

110 A standard solution was analyzed as a quality control sample for every 10 samples.

Water-soluble ions: Sample sections and blank filters were extracted with 10 mL Milli-Q water ($\geq 18.0\text{ M}\Omega\cdot\text{cm}$) using ultrasonication for 40 min at 0° C followed by filtration through a $0.45\text{ }\mu\text{m}$ pore diameter filter, then stored at $\sim 4^{\circ}$ C until analysis in 3 days. Water-soluble ionic species, including Na⁺, NH₄⁺, K⁺, Mg²⁺, Ca²⁺, Cl⁻, NO₃⁻, SO₄²⁻ and C₂O₄²⁻, were analyzed using a Dionex ICS-3000 ion chromatography. To monitor instrumental precision/accuracy and quantify background contamination over the analytical sequence, blank filter solutions and standard solutions were analyzed every 10 samples. See Text S1b for additional QA/QC details.

115

OC and EC: 2.0 cm^2 section of samples and blank filters were analyzed by a Sunset OC/EC analyzer using NIOSH protocol (Wu et al., 2016). The data obtained were calibrated with a standard curve. Detailed information is described in Text S1c.

2.3 Other data and backward trajectories

120 Meteorological parameters during the sample collection periods, including relative humidity (RH), wind speed (WS) and wind
direction, were obtained from the shipboard measurements and Qingdao Meteorological Bureau, and monitoring data of
gaseous pollutants, including SO₂, NO₂, O₃, and CO, were from China National Environmental Monitoring Centre
(<http://www.cnemc.cn/>, <https://quotsoft.net/air/>).

The Hybrid Single-Particle Lagrangian Integrated Trajectory (HYSPLIT) model (PC v4.8) developed by the National Oceanic
125 and Atmospheric Administration Air Resources Laboratory (NOAA-ARL) (Draxler and Rolph, 2014) was employed to
reconstruct the three-dimensional 72-h backward trajectories. This was done to identify distinct air mass source regions and
their transport paths. The starting point for the trajectory calculations was set at an altitude of 300 m above the ground level.
The calculations were performed with the vertical velocity calculation method and archived Global Data Assimilation System
(GDAS) meteorological data.

130 2.4 Positive matrix factorization receptor model

The Positive Matrix Factorization (PMF) model is a widely used receptor model to resolve pollution sources and quantify the
source contributions to ambient particulate matter concentrations (Paatero and Tapper, 1994). It decomposes the measured
data matrix into factor profile, contribution, and residual matrix. In this study, the Environmental Protection Agency (EPA)
PMF version 5.0 was utilized for analysis (Norris et al., 2014).

135 In this study, the mass concentrations of 12 elements (V, Cr, Mn, Fe, Ni, Co, Cu, Zn, As, Cd, Ba and Pb), 9 water-soluble ions
(Na⁺, NH₄⁺, K⁺, Mg²⁺, Ca²⁺, Cl⁻, NO₃⁻, SO₄²⁻ and C₂O₄²⁻), and OC/EC from both Qingdao and cruise campaigns (81 samples)
were input to the PMF analysis. Multiple factors ranging from 6 to 10 were thoroughly evaluated to determine the optimal
solution. The stability and reliability of the factor solutions were assessed using the displacement (DISP) and bootstrap (BS)
uncertainty estimation methods (Norris et al., 2014). Ultimately, an 8-factor solution emerged as the most robust and
140 interpretable. In contrast, the 7-factor solution failed to distinguish the industrial emissions from dust (Fig.S1a). The 9-factor
solution tended to resolve an additional factor; however, it exhibited relatively low BS mapping values (58%, 67%, and 73%)
for several factors (Fig.S1b and Table S2). The 8-factor solution demonstrated the highest stability. The mapping percentages
using the BS uncertainty method exceeded 80% for all factors (Table S3), surpassing the performances of the 7-factor and 9-
factor solutions (Tables S4 and S2). Moreover, the DISP analysis showed no occurrences of factor swapping and no reduction
145 in the model fit statistic Q (both %dQ and the error code were 0), further validating the stability and interpretation of the 8-
factor solution. Detailed information on the PMF performance, including time series analysis, can be found in Text S3.

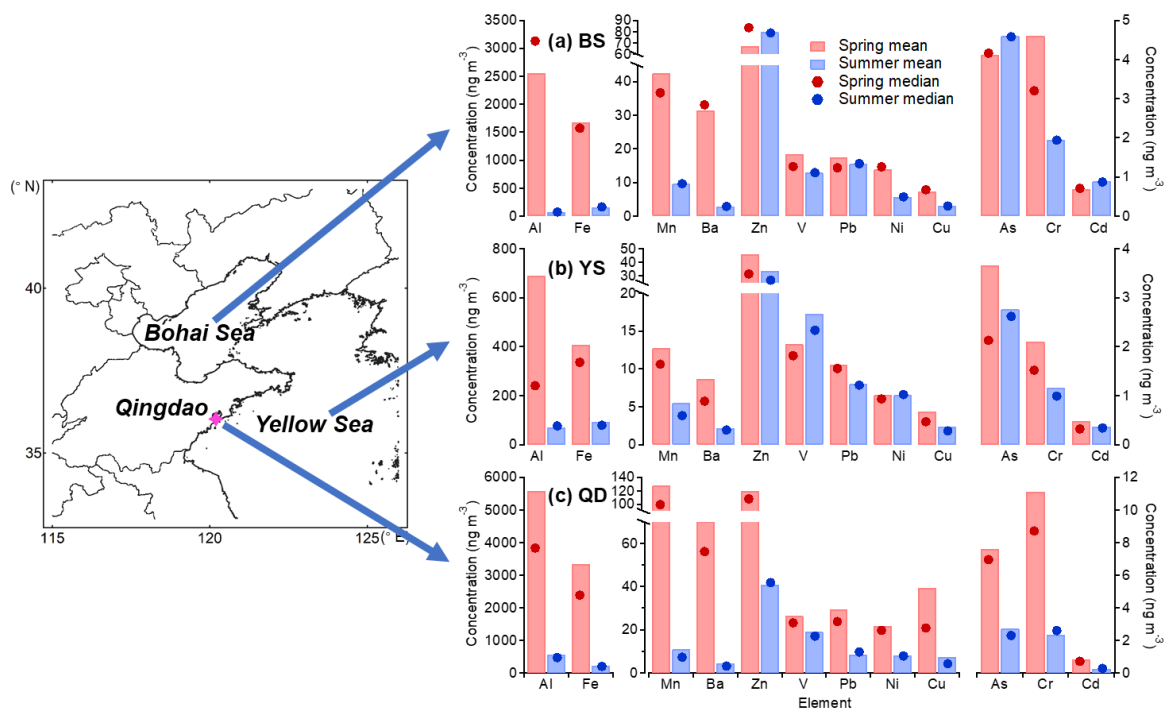
3 Spatiotemporal distributions of trace elements

Figure 2, Tables S5 and S6 summarize the overall average concentrations of elements. Over the BS and YS, the predominant
trace elements were Al, Fe, and Zn, with concentrations (average ± standard deviation) of 1043.2 ± 1031.0 ng m⁻³, 648.6 ±

150 654.8 ng m⁻³, and 49.9 ± 75.0 ng m⁻³ in spring, and 71.1 ± 19.0 ng m⁻³, 109.8 ± 51.4 ng m⁻³, and 44.9 ± 30.2 ng m⁻³ in summer, followed by Mn (spring) and V (summer) respectively. In the coastal city, the dominant trace elements were Al and Fe, with average concentrations of 5573.5 ± 5641.1 and 3347.3 ± 3249.3 ng m⁻³ in spring and 572.9 ± 395.4 and 228.3 ± 211.7 ng m⁻³ in summer, followed by Mn in spring and Zn in summer, respectively (Fig.2c). Among the measured anthropogenic trace elements (e.g., Pb, Cu, As, Cd), Zn was the most abundant in both marine and coastal environments, with its anthropogenic origin confirmed by a high enrichment factor (Text S2 and Fig.S2) (Taylor, 1964). Except for V, element concentrations during summer in Qingdao were lower than those reported by Li et al. (2018) during summer 2016. In this study, V and Ni, as representative tracers of emissions from heavy oil combustion, indicated a higher influence from this source during the campaigns (Li et al., 2020; Zhang et al., 2019b; Zhao et al., 2013).

All elements displayed notably higher concentrations in Qingdao compared to the marine area in spring. However, the discrepancy in concentrations of V, As, and Cd between land and sea was relatively smaller than those of other elements (Fig.2). The YS region recorded the lowest concentrations for most elements in both spring and summer. Conversely, Zn, As, and Cd exhibited elevated levels over the ocean in summer (Fig.S3b), highlighting the significant impact of transported primary anthropogenic emissions on marine aerosol composition. Notably, a severe pollution event (sample SU005, 1-2 August 2018) under stagnant meteorological conditions ($WS < 2 \text{ m s}^{-1}$) led to a pronounced concentration peak of these elements over marine areas. Back trajectory analysis indicates that the air masses originated from the industrial emissions and coal combustion-intensive regions of the BS and Liaodong Peninsula (Fig.S4d), further underscoring the significant impact of transported primary anthropogenic emissions on marine aerosol composition. Given the high sensitivity of the mean to such an extreme outlier, particularly with the limited sample size, this sample was excluded from both the calculation of average values and subsequent PMF analysis.

170 Seasonally, concentrations of Al, Fe, Mn, and Ba over the BS and YS in spring were 4–35 times and 2–10 times higher than those in summer, respectively. This distinct seasonality can be attributed to dust storms, a frequent phenomenon in northern China during spring (Li et al., 2019). In contrast, Zn, As, and Cd displayed slightly higher concentrations over the BS in summer than in spring, suggesting anthropogenic emissions in the Circum-Bohai-Sea (CBS) region (a geographic area encompassing the land and coastal zones surrounding the BS in China, it includes, but is not limited to, the Bohai Rim) (Polissar et al., 2001). Conversely, V and Pb exhibited no discernible seasonal variations, likely due to the consistent anthropogenic emissions such as industrial and residual oil combustion emissions (Wu et al., 2017). In Qingdao, concentrations of all these elements were notably higher in spring compared to summer (Fig.2c).



180 **Figure 2: Concentrations of trace elements (ng m^{-3}) over the (a) BS, (b) YS, and (c) Qingdao during the campaigns in 2018. The bars represent the time-weighted (hereafter) average, and the circles represent the median.**

We compared our results to other literature data on the concentrations of selected elements in various oceanic regions and typical megacities in China (Tables S5 and S6) (Qi and Zhou, 2021). Notably, elemental concentrations over the YS in this study were significantly lower than those observed during spring 2011 (Zhao et al., 2015). This decrease suggests a potential reduction in the overall aerosol burden transported to the YS in 2018. It could be a consequence of interannual variations in continental outflow and/or the effectiveness of emission control policies and environmental remediation measures, with the decline in anthropogenic tracers (e.g., Zn, V, Ni, As) providing specific support for the potential role of emission controls. When comparing with spring 2018 ECS sampling data (Sun et al., 2022), a distinct north-to-south decline in the concentrations of mineral elements (Al, Fe, Mn, Ba) and anthropogenic heavy metals (e.g., Zn, Pb) was observed. This spatial pattern suggests that both dust-derived and anthropogenic pollutants, transported via the westerly winds, exert progressively weaker influences on marine aerosols from northern to southern coastal regions (Zhao et al., 2015). Only a few measurements in island were collected in summer (Yuan et al., 2023), and comparison with concentrations in this study showed no order-of-magnitude differences for most elements.

In Qingdao, most crustal elements, such as Fe and Mn, exhibited higher concentrations in spring and lower concentrations in summer than the annual average concentrations reported in Beijing, Shanghai, and Guangzhou, the typical megacities in China (Table S6) (Chen et al., 2008; Yang et al., 2011). This pattern highlighted the pronounced seasonality of crustal influence in Qingdao, with spring being strongly impacted by dust events, while the input of crustal dust was substantially weakened in

summer. Anthropogenic elements such as Zn, Pb, As, Cr, and Cd, which are typically associated with sources like coal combustion, non-ferrous metal smelting, and various industrial processes (Borai et al., 2002; Chen et al., 2013; Karar et al., 2006; Li et al., 2015; Li et al., 2020), were consistently at lower levels in Qingdao than in the three megacities, indicating a lower overall burden from these anthropogenic sources in Qingdao. Notwithstanding the differences in sampling year and season, V concentrations in Qingdao were 2–3 times higher than those in Shanghai (Chen et al., 2008), suggesting a more severe pollution from ship emissions or other residual oil combustions in Qingdao. However, the differences in sampling times need consideration. Sect. 4.2.3 explores the impact of vessel emission control policies on the ship emission aerosols.

4 Discussions

4.1 Source apportionment of PM_{2.5}

Eight factors were identified by PMF. The resolved factor profiles and time series are presented in Fig.3 and Fig.4 respectively. The mean concentrations and the relative contributions of each factor are displayed in Fig.5. The characteristics of the determined aerosol sources are as follows.

Factor 1 was identified as the secondary nitrate factor, characterized by high loadings of NO₃⁻, NH₄⁺ and Cl⁻ (Fig.3) (Wu et al., 2017; B. Xu et al., 2023). This factor contributed a significant proportion of fine particles in both Qingdao and marine environments, accounting for 34.9% and 16.9% of PM_{2.5} mass respectively (Fig.5b). Notably, Factor 1 displayed an enhanced influence during nighttime (Fig.S5). To help validate the source of this factor, its time-series contribution was compared to ambient gas measurement data (Text S3, Fig.4, and Table S7). It correlated with NO₂ ($r = 0.45$, $p < 0.01$) and CO ($r = 0.39$, $p < 0.01$). This could potentially be indicative of the nocturnal heterogeneous reaction formation or subsequent regional transport (Wang et al., 2018).

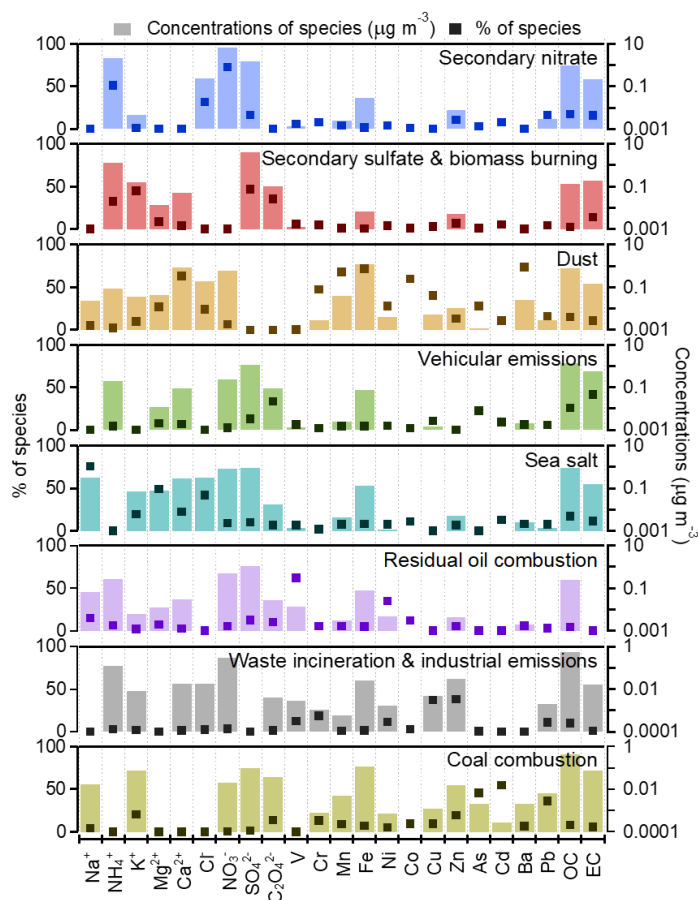


Figure 3: PMF resolved source profiles (dark points represent the percentages and light rectangles represent the concentrations of each species in each factor) of the 8-factor solution.

Factor 2 was recognized as the secondary sulfate and biomass burning (sulfate & BB) factor, marked by high SO_4^{2-} , K^+ , NH_4^+ and oxalate (Wu et al., 2017; B. Xu et al., 2023). This factor accounted for 19.4% and 24.3% of the $\text{PM}_{2.5}$ mass in Qingdao and marine regions respectively. The notable presence of K^+ , oxalate, and some EC and Zn in this factor suggested the possible mixing with emissions from biomass burning (Wang et al., 2018; Zhu et al., 2022). Factor 2 exhibited correlations with CO ($r = 0.54$, $p < 0.01$) and RH ($r = 0.36$, $p < 0.01$). CO serves as a key tracer of primary incomplete combustion processes (Zhang et al., 2017). The strong interconnection between sulfate and oxalate can be ascribed to their similar liquid phase formation mechanisms (Yu et al., 2005; Zhou et al., 2015).

Factor 3, identified as the dust factor, was characterized by high loadings of crustal species, including Ba, Fe, Mn and Ca^{2+} (Fig.3) (Amil et al., 2016; Gugamsetty et al., 2012; Mustafa et al., 2014). A significant portion of Co was also apportioned to Factor 3, denoting its crustal origin (Wu et al., 2023). In Qingdao, the time series of Factor 3 exhibited distinct peaks on 29–30 March, 3, 6, 10–11, and 15 April 2018 (Fig.4a), each coinciding with documented springtime Asian dust events (Li et al., 2023; Li et al., 2019). Diurnally, Factor 3 exhibited a moderate positive correlation with WS ($r = 0.43$, $p < 0.05$) in Qingdao

in spring. Throughout the entire sampling campaign, it maintained a strong negative correlation with RH ($r = -0.72$, $p < 0.01$; Table S7) in Qingdao. These correlations suggested the influence of meteorological conditions, consistent with the inherently arid nature of dusty air masses. Factor 3 accounted for 13.6% of the total $PM_{2.5}$ mass at coastal site and diminished to 1.7% within the marine environments (Fig.5b).

Factor 4 was identified as the vehicular emissions factor, characterized by significant apportionments for EC and OC, contributing 10.4% to the total Qingdao aerosol mass and 17.6% to the marine aerosols. OC and EC are major pollutants stemming from gasoline and diesel combustion (Liu et al., 2016; Liu et al., 2020). The presence of Cu was likely due to additives in fuel/lubricant combustion, brake linings and tire wear (Gu et al., 2011; Lee et al., 2006; Pant and Harrison, 2013), further supporting this identification. During summertime, vehicular emissions correlated strongly and positively with NO_2 ($r = 0.78$, $p < 0.01$). Throughout the sampling campaign, the factor correlated positively with CO ($r = 0.30$, $p < 0.05$) and negatively with O_3 ($r = -0.37$, $p < 0.01$). These relationships underscored the chemical interplay where O_3 is reduced by NO to generate NO_2 .

Factor 5 was characterized by high concentrations of sea salt components, including Na^+ , Mg^{2+} and Cl^- , and showed a positive correlation with WS ($r = 0.35$, $p < 0.01$) and a strong negative correlation with RH ($r = -0.63$, $p < 0.01$) (Sharma et al., 2016; Zhang et al., 2018). This factor aligned with the generation of sea salt aerosols via wind-induced disturbance on the ocean surface (Prijith et al., 2014). At the coastal site, the augmented concentrations during the daytime aligned with the sea-land breeze patterns (Fig.S5). Time series analysis indicated that Factor 5 had a prevalent influence over the BS and YS (Fig.4). Notably, the concurrent peak concentrations in the time series of Factor 5 and Factor 3 observed in Qingdao during spring, strongly suggested the mixing of sea salt and dust during atmospheric transport. This co-variation is consistent with the prevailing westerly/northwesterly winds (Fig.1) facilitate the transport of both continental dust and sea salt aerosols (generated over the BS and YS regions) to the coastal sampling site. To further support this transport mechanism, backward trajectories are presented in Fig.S6 for a representative marine sample (SP012, exhibiting the highest sea salt source concentration) and its corresponding Qingdao samples during the same period. These trajectories clearly illustrate that the air masses originated from the YS and approached Qingdao from the west prior to their arrival at the sampling site. Additionally, high wind speeds associated with dust events can also generate sea salt aerosols (Feng et al., 2017), which represents a primary driver of the observed similarity in the temporal profiles of dust and sea salt. On average, the sea salt factor contributed 9.9% to $PM_{2.5}$ mass at the Qingdao site and 22.1% in marine $PM_{2.5}$ samples.

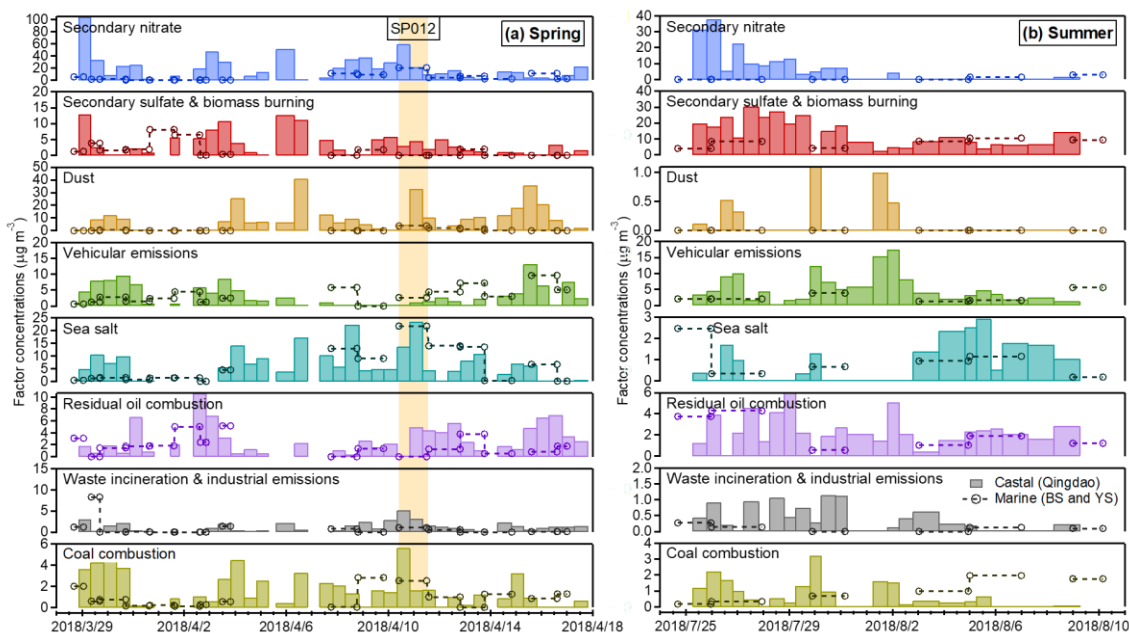
Factor 6, the residual oil combustion factor, was characterized by high apportionments of V and Ni (Wu et al., 2020), contributing 6.6% and 9.0% to the total $PM_{2.5}$ mass in Qingdao and BS and YS areas, respectively. The cargo handling capacity of Qingdao port reached 542.5 million tons in 2018, ranking fourth among the main ports of China (data obtained from China Statistical Yearbook, 2018, <https://data.stats.gov.cn/easyquery.htm?cn=C01>). The contributions of Factor 6 highlighted the significant influence of shipping traffic on both the coastal city Qingdao and the BS and YS areas. It showed a positive correlation with SO_2 ($r = 0.38$, $p < 0.01$) (Table S7), further validating its association with ship emissions (Zhang et al., 2019b).

265 Factor 7 was defined as the waste incineration & industrial emissions factor (WI & IE). It exhibited substantial loadings of heavy metals such as Zn, Cu, Cr, and Pb, which are tracers of waste incineration and industrial activities, including metallurgical smelting, oil mining, and the production of cement, plastic, pigment, chemical and building materials (Borai et al., 2002; Karar et al., 2006; Li et al., 2012; Tian et al., 2012; Wang et al., 2018). Its correlations with NO₂ (r = 0.50, p < 0.01) and SO₂ (r = 0.31, p < 0.05) underscored its industrial origins, although it is a minor contributor to total PM_{2.5} (3.1% in Qingdao and 1.5% in the BS and YS areas, as shown in Table S7).

270 Factor 8 was identified as the coal combustion factor. This attribution was robustly supported by the enrichment of well-documented coal combustion tracers of As, Cd and Pb, elements consistently linked to coal-fired emissions (Chang et al., 2018; Li et al., 2020; Rai et al., 2016; Zhang et al., 2011; Zhang et al., 2008). Furthermore, the factor exhibited a statistically significant correlation with SO₂ (r = 0.35, p < 0.01), a primary gaseous co-emission from coal combustion (Lin et al., 2022).

275 This coal combustion factor contributed modestly to the total PM_{2.5} mass but showed notable spatial variability: 2.1% at coastal (Qingdao) site and 4.8% in marine PM_{2.5} samples, with marine contributions exceedingly twice the coastal value. The spatial distributions of coal-fired power plants, PM_{2.5} emissions by coal-fired power plants, and atmospheric As concentration in China collectively indicated that the coal combustion factor likely originated from transport (Fig.S7) (Tian et al., 2014; Wang et al., 2016; Zhang et al., 2020). In particular, the dense concentration of coal-fired power plants along the coastline serves as a persistent source of coal-burning aerosols over the sea.

280 a persistent source of coal-burning aerosols over the sea. Furthermore, despite its limited contribution to PM_{2.5} mass, its contribution to heavy metal concentrations is substantial, which will be discussed in detail in Sect. 4.3.



285 **Figure 4: Time series of individual PMF factor concentrations for PM_{2.5} in (a) spring and (b) summer. “SP012” marked in (a) shows the factor concentrations during the sampling period of sample SP012. The detailed procedure for converting the model’s factor contribution output to concentrations is provided in Text S3.**

4.2 Difference and linkage in source contributions of PM_{2.5} between coastal and marine environments

4.2.1 Spring westerly transport enhances anthropogenic inputs in marine areas

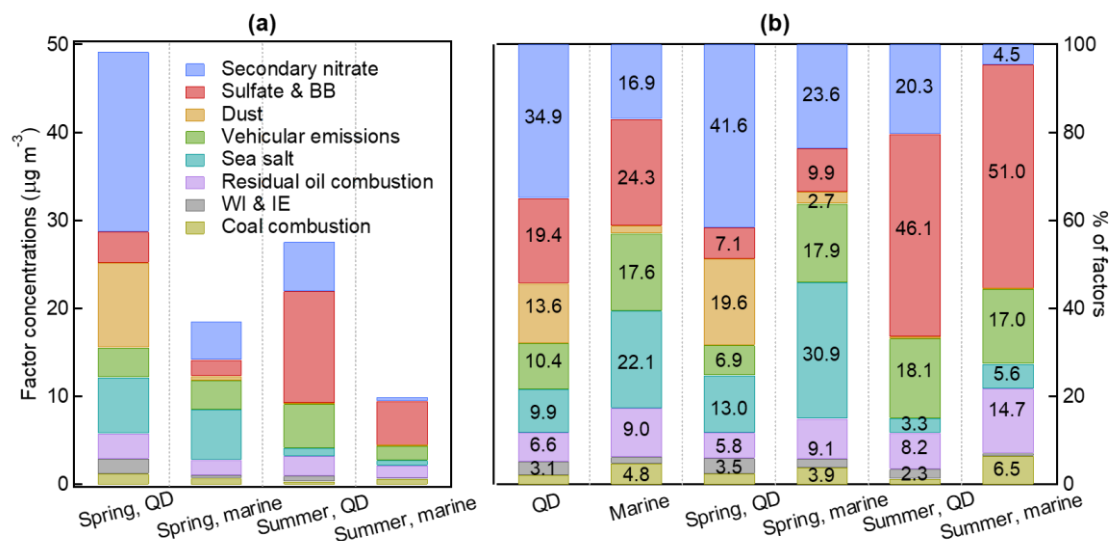
Distinct differences in PM_{2.5} source apportionment were observed between the coastal and marine environments during spring. Secondary nitrate, dust, and WI & IE exhibited significantly lower concentrations and relative contributions in marine environments compared to the coastal site. Specifically, secondary nitrate was the predominant contributor at the coastal site, accounting for 41.6% (20.4 $\mu\text{g m}^{-3}$) of PM_{2.5} mass. In contrast, its contribution was notably lower in the marine area (23.6% , 4.4 $\mu\text{g m}^{-3}$; Fig.5). This disparity was driven by the divergence in the air masses transport pathways. Air masses arriving at Qingdao (spring clusters E, S, W and summer cluster L) contained higher concentrations of secondary components like NO₃⁻ and NH₄⁺ (land-based species), which did not fully extend to marine areas (Fig.S4a and c, and Table S8). As NO₃⁻ and NH₄⁺ are primarily associated with terrestrial sources, their influence is more significant in Qingdao.

Dust, the second largest contributor in spring, accounted for 19.6% (9.7 $\mu\text{g m}^{-3}$) in Qingdao but sharply reduced to 2.7% (0.5 $\mu\text{g m}^{-3}$) over the BS and YS. Dust particles with larger diameters are more likely to be removed through inertial and gravitational settling processes during transport (Gu et al., 2011; Vu et al., 2015; Zhao et al., 2015), leading to the rapid sedimentation and reduced concentration in remote marine environments (Baker and Jickells, 2006; Ma et al., 2023). The WI & IE factor also showed lower contributions in the marine area (2.0%) compared to the coastal site (3.5%).

Sea salt, sulfate & BB, coal combustion, vehicular emissions and residual oil combustion showed higher contributions in the marine area, despite lower or comparable absolute concentrations to the coastal site (Fig.5). Sea salt contributions were 30.9% in the marine area, versus 13.0% at the coastal site, consistent with the fact of its marine origin. Furthermore, its temporal peaks at Qingdao closely resembled those of the dust factor (Fig.4a). It is hypothesized that during dust events, sea salt may mix with the transported dust, making the two factors difficult to distinguish and leading to the higher concentration of sea salt at Qingdao (6.4 $\mu\text{g m}^{-3}$) compared to those over the marine area (5.7 $\mu\text{g m}^{-3}$).

On the one hand, increased RH in marine air favored the formation of sulfate and oxalate through liquid-phase reactions (Zhang et al., 2019a; Zhou et al., 2015), enhancing sulfate & BB contribution in the marine atmosphere (9.9%) compared to the coastal site (7.1%). On the other hand, small-sized particles from biomass burning and coal combustion are more effectively transported to marine areas (Gu et al., 2011; Vu et al., 2015). The vehicular emissions, accounting for 17.9% in marine areas (Fig.5b), had nearly identical average concentrations in both Qingdao and marine environments (3.4 and 3.3 $\mu\text{g m}^{-3}$, respectively) (Fig.5a). Characterized by small EC-rich particles, these vehicular emissions can be easily transported to remote areas (Gu et al., 2011; Vu et al., 2015). As shown in Figs.4a, S8a and c, time series peaks of this factor over the ocean coincided with the samples collected from air masses originating in northern and central China, i.e., samples SP010, SP014, and SP017.

Residual oil combustion exhibited a lower average concentration in marine areas (1.7 $\mu\text{g m}^{-3}$) than Qingdao (2.9 $\mu\text{g m}^{-3}$), indicating the influence of ships and ports emissions on coastal urban areas. Unlike the WI & IE factor, these four anthropogenic factors demonstrated that varying transport paths, particle size, and source proximity could affect land-sea distribution patterns of their contributions.



320 **Figure 5:** The averaged (a) concentrations and (b) relative percentage contributions of identified source factors to $\text{PM}_{2.5}$ as determined by PMF analysis. Sulfate & BB refers to sulfate & biomass burning. WI & IE denotes waste incineration & industrial emissions. “marine” refers to the BS and YS.

4.2.2 Summer biomass burning and vehicular emissions dominate marine source contributions

325 Similar spatial land-sea distribution patterns were observed for secondary nitrate, dust, WI & IE, as well as sulfate & BB in summer. However, the dominant contributor shifted from secondary nitrate in spring to sulfate & BB in summer, indicating decreased nitrate contributions during the warmer season. This reduction was attributed to the thermal decomposition of NH_4NO_3 under high summer temperatures and enhanced secondary sulfate facilitated by photochemical reactions with the high temperature and sufficient light (Wu et al., 2017).

330 Unlike in spring, summer data revealed higher concentrations and contributions of vehicular emissions at the coastal site ($5.0 \mu\text{g m}^{-3}$, 18.1%) compared to the BS and YS ($1.7 \mu\text{g m}^{-3}$, 17.0%) (Fig.5). This difference could be ascribed to the seasonal variations in pollutants transport direction, driven by the summer southeasterly winds, altering typical land to sea trajectories. Similarly, sea salt concentrations were higher at the coastal site ($0.9 \mu\text{g m}^{-3}$) compared to marine areas ($0.6 \mu\text{g m}^{-3}$), suggesting that summer southeasterly winds facilitate marine aerosol transfer inland, thereby influencing the air quality of coastal urban areas (Figs.S4c, d, and S8d). The coal combustion factor also showed a more pronounced contribution over the marine area 335 ($0.6 \mu\text{g m}^{-3}$, 6.5%) than at the coastal site ($0.4 \mu\text{g m}^{-3}$, 1.3%). This variation was attributed to elevated concentrations of trace elements in marine aerosols during summer.

4.2.3 Changes over the past decade

Comparative analysis of particulate matter source apportionment between the present study and earlier work (Wu et al., 2017) suggested evolving trends in source contributions over the past decade. Notably, statistical comparison is not feasible due to

340 the lack of primary data from the earlier study. The observed differences showed an increase in the fraction of secondary nitrate (from 25.2% to 34.9%), a decrease in sulfate (& BB) (from 25.7% to 19.4%), and minimal change in vehicular emissions contribution (from 10.0% to 10.4%), accompanied by an elevation in the mass concentrations of Ni and V. These observed variations were consistent with the impacts of evolving environmental regulations and the transformation in the energy structure over the past decade.

345 Another interesting trend is the contribution from residual oil combustion. As a coastal city, Qingdao experiences heavy shipping traffic. Results from a PMF analysis conducted from August 2018 to May 2019 near the Qingdao Port indicated that marine vessel emissions were the primary contributor (25.1%), with the YS and BS as potential source regions (Bie et al., 2021). In this study, residual oil combustion accounted for 6.6% at the coastal site and 11.1% over the marine area. The cargo handling capacity of Qingdao ports in 2017 was approximately double that of 2007 (China Statistical Yearbook, 2018 and 350 2008, <https://data.stats.gov.cn/easyquery.htm?cn=C01>), underscoring the significant impact of ship emissions.

The implementation of “domestic emission control areas” (DECAs) in China signified a significant regulatory shift to address air quality concerns. Commencing on January 1, 2017, ships berthed at core ports in three designated regions (the Pearl River Delta, the Yangtze River Delta, and the Bohai Rim) were mandated to use fuel with a sulfur content not exceeding 0.5% (DECA 1.0) (Zhang et al., 2019b). This regulation was further expanded on January 1, 2019 to require vessels operating within 355 12 nautical miles of the coastline to adhere to the same low sulfur criteria (DECA 2.0) (Yu et al., 2021). The transition to low-sulfur fuels led to a significant increase in the Ni/V ratio of emitted aerosols. This phenomenon was primarily caused by the desulfurization of fuels which removed V much more efficiently than Ni, thereby increasing the Ni/V ratio in the fuel itself, which is then reflected in the combustion emissions (Yu et al., 2021). In Shanghai, the Ni/V ratio in ship emitted particles derived from PMF increased from 0.34 to 0.45 between DECA 1.0 and DECA 2.0, reaching 2.14 in 2020 (Yu et al., 2021). In 360 the present study, the Ni/V ratio for residual oil combustion aerosols resolved by PMF was 0.37, aligning with DECA 1.0 levels. Notably, Bie et al. (2021) reported a Ni/V ratio of 2.17 in 2019 near the Qingdao Port, confirming DECA policy effectiveness. The lower Ni/V ratio (0.37) in our study suggested residual oil combustion pollutants in the study area may still include higher-sulfur fuel signatures, potentially from regional transport rather than strictly regulated local shipping..

4.2.4 Comparison with source apportionment studies in other marginal seas of the Western Pacific

365 We compared the source apportionment results obtained over the BS and YS in this study with those from studies conducted over the offshore eastern China Sea (OECS), around the Taiwan Island (China), and over the South China Sea (SCS) (Sun et al., 2022; Yen et al., 2022a; Yen et al., 2022b). These sea areas all belong to the marginal seas of the Western Pacific, sharing the common influence of the East Asian monsoon and continental outflows, yet exhibiting differences in the types of pollution sources and their respective contributions.

370 Over the marginal seas of the Western Pacific, PM_{2.5} sources were generally dominated by secondary inorganic aerosols, dust (including crustal or fugitive dust as reported in other studies), sea salt (including marine source or oceanic spray), and specific anthropogenic emissions. Among these, secondary aerosols (dominated by nitrate and/or sulfate) and sea salt made particularly

375 prominent contributions. In studies conducted over the OECS, secondary formation (22.9%) and combustion source (30.6%) were reported to make significant contributions (Sun et al., 2022; Fig.S9c), which is qualitatively similar to our findings. The notable contribution of sea salt in this work is also consistent with its important role reported in other sea areas, such as 18.6–30.2% around the Taiwan Island and 5.6–29.5% over the SCS (Yen et al., 2022a; Yen et al., 2022b; Fig.S9a, b, and d). In terms of the apportionment results for specific anthropogenic sources, the PM_{2.5} sources over the BS and YS exhibited a stronger continental signal, including the identification of more distinct factors for industrial processes and coal combustion. This characteristic was less pronounced over the more southerly sea areas, reflecting the profound impact of the industrial structure and coal-dominated energy mix of Northern China on the marine regions. Furthermore, vehicular emissions constituted a major and stable pollution source over the BS and YS, aligning with the high contribution (24.5%) reported in the OECS study (Sun et al., 2022). In contrast, studies conducted around the Taiwan Island and over the SCS commonly resolved a mixed factor combining ship and vehicular emissions, which was dominant (17.4–41.2%) (Yen et al., 2022a; Yen et al., 2022b). This suggested that over the BS and YS, traffic and shipping emissions were more readily separated, likely due to the differing coastal urban agglomerations and distinct emission patterns. The comparison revealed the regional commonalities of PM_{2.5} sources in the Western Pacific marginal seas and their spatial divergence under the influence of local emissions.

4.3 Source contributions of individual elements

390 This study revealed clear disparities in the source contributions to the ten essential elements across terrestrial and marine regions, mirroring the spatial distribution patterns seen in PM_{2.5} (Fig.6, Fig.S10, Table S9 and S10). The influence of dust and WI & IE sources decreased, whereas coal combustion, vehicular emissions (in spring) and sea salt exhibited enhanced contributions to elements over the marine area.

4.3.1 Fe, Mn and Cr

395 Atmospheric aerosols containing Fe and Mn are crucial for marine biogeochemistry and ecosystem dynamics. As a limiting nutrient, Fe is closely coupled with sulfur cycles (e.g., via dimethyl sulfide production/processing) in both the atmosphere and ocean, triggering phytoplankton blooms, and enhancing carbon dioxide (CO₂) sequestration through the global carbon cycle (Shi et al., 2012; Zhuang et al., 1992). Similarly, Mn serves as an essential cofactor for enzymes involved in photosynthesis and other biochemical processes, making it vital for marine organisms, and its deficiency directly impacts the growth rate of phytoplankton (Morel and Price, 2003; Hawco et al., 2022).

400 In spring, dust was the dominant source of Fe and Mn in Qingdao, contributing 81.6% and 78.6% to the total Fe and Mn, respectively (Fig.6a and b). However, marine aerosols exhibited significantly increased contributions from vehicular emissions (11.0% and 10.6% for Fe and Mn, respectively) and coal combustion (16.2% and 19.5%). Coal combustion contributed 92.4 ng m⁻³ Fe and 4.0 ng m⁻³ Mn to the marine atmosphere in spring, while dust contributed 145.2 ng m⁻³ Fe and 4.8 ng m⁻³ Mn (Fig.S10). In summer, coal combustion became the primary contributor to marine Fe and Mn (43.2% and 46.5%, respectively),

405 exceeding Qingdao contributions by 3 times. The absolute concentration from coal combustion was 82.8 ng m^{-3} for Fe and 3.6 ng m^{-3} for Mn. It should be noted that the PMF-resolved total Fe concentration in marine aerosols during summer was higher than the measured value, indicating a proportional overestimation in absolute source contributions. However, the strong correlation between PMF-simulated and measured Fe concentrations confirms the robustness of the relative source apportionment. Detailed discussion on this discrepancy and its implications is provided in Text S3 and Fig.S11a. This shift
410 highlights the long-range transport of fine anthropogenic particles to marine regions, enriching aerosols with pollution-derived elements. The comparison of source concentrations revealed that coal combustion was a substantial source of Fe to the marine aerosols in both seasons, with its importance increasing in summer. Nevertheless, in terms of absolute concentration, the spring contribution to Fe was slightly higher than that in summer. It is noteworthy that residual oil combustion was also a discernible source for Fe and Mn in summer (contributing 26.1%, 50.0 ng m^{-3} and 24.4%, 1.9 ng m^{-3} respectively in marine areas).
415 Southeasterly winds transported ship-derived pollutants coastward, markedly increasing the relative contributions of Fe (24.1%) and Mn (22.9%) in Qingdao compared to spring (2.8% and 3.1%, respectively). However, from the perspective of absolute concentration, the contributions of residual oil combustion to Fe and Mn in Qingdao remained lower in summer (77.8 and 2.9 ng m^{-3} , respectively) than in spring (98.7 and 3.7 ng m^{-3}).

These findings align with previous studies: Chen et al. (2024) reported dust as the predominant source of Fe (88%) in Qingdao
420 during spring (Chen et al., 2024), while Zhang et al. (2024) observed substantial contributions from both dust (68.6%) and coal combustion (21.2%) in the YS, ECS, and Northwest Pacific. The findings regarding Mn in Beijing align with our analysis for Qingdao, where dust served as the primary source during spring, but shifted to industrial emissions in summer (Yang et al., 2022).

Notably, our source apportionment revealed a significant contribution of anthropogenic combustion to total Fe (Fig.6a). Such
425 anthropogenic Fe was reported to typically exhibit higher solubility, in comparison with Fe from natural sources such as mineral dust (Ito et al., 2021; Sun et al., 2024). The greater solubility and consequent higher efficiency in enhancing productivity can be explained by the physicochemical properties of the particles. Combustion processes emit Fe in finer particles with a larger surface-area-to-volume ratio. Such particles are more susceptible to atmospheric acid processing, which efficiently converts insoluble Fe into soluble forms (Shi et al., 2012; Ito et al., 2021). In contrast, Fe in natural mineral dust is
430 largely encapsulated within refractory aluminosilicate minerals, making Fe less available for solubilization.

Furthermore, sea salt contributed 33.6% to Fe and 29.7% to Mn in marine aerosols during spring, suggesting mixing between
435 crustal species or Fe/Mn from other sources with sea spray aerosols (SSAs) (Geng et al., 2014; Hilario et al., 2020). Furthermore, sea salt contributed 33.6% to Fe and 29.7% to Mn in marine aerosols during spring, suggesting mixing between crustal species or Fe/Mn from other sources with sea spray aerosols (SSAs) (Geng et al., 2014; Hilario et al., 2020). Internal mixing between mineral dust and sea salt has been observed in various regions, such as the marine atmosphere of East Asia, the Amazon basin, the eastern North Atlantic, the Southern Hemisphere ocean, and the Pacific Ocean, through electron microscopic analyses (Andreae et al., 1986; Okada et al., 1990; Zhang et al., 2003; Zhang et al., 2006; Wagener et al., 2008; Hsu et al., 2010; Adachi et al., 2020; Knopf et al., 2022; Kwak et al., 2022). However, the net effect of this mixing on Fe

bioavailability appeared complex and was not necessarily positive (Hsu et al., 2010; Sakata et al., 2022; Wu et al., 2023). Hsu et al. (2010) reported a negative correlation between sea salt and fractional Fe solubility, likely mediated via pH effects (Spokes and Jickells, 1996; Desboeufs et al., 1999). Proposed mechanisms include SSA buffering solution acidity to reduce particle solubility, and competing with dust particles for acid uptake, thereby inhibiting heterogeneous acid processing (Hsu et al., 2007). It should be noted, however, that Hsu et al. (2010) used TSP samples, whereas recent mesocosm experiments indicate that submicron SSA may rapidly acidify to pH 2.0 via evaporation, acidic gas uptake, and/or proton displacement from organics by Na⁺ (Angle et al., 2021). Thus, the actual acidity of ambient submicron SSA may remain sufficiently high to promote dissolution. Moreover, organic constituents in SSAs (e.g. Humic-like Substances, HULIS) may primarily stabilize existing soluble Fe rather than enhance Fe dissolution, although Wu et al. (2023) demonstrated that strong organic ligands can significantly facilitate and sustain Fe release. Therefore, the overall impact of SSA mixing on Fe bioavailability likely depends on specific marine environmental conditions and requires future investigation.

The source pattern of Cr shared some similarities with that of Fe and Mn in spring (Fig.6c). Marine aerosols exhibited a pronounced increase in coal combustion contributions (30.0% in spring and 49.1% in summer) compared to Qingdao particles, likely due to emissions from coastal power plants transported seaward. WI & IE was the second-largest contributor to Cr in Qingdao during spring and the largest contributor during summer, qualitatively similar to the findings of Yang et al. (2022) for Beijing, although the industrial emissions contribution levels they reported (41%–77%) were substantially higher than those in our study (15.3% in spring, 27.3% in summer).

4.3.2 Ni, Cu, Zn, V and Cd

Ni, Cu, Zn, and Cd can influence phytoplankton growth dynamics, modify marine biotic community structure, and affect carbon sequestration processes, functioning either as enzyme cofactors or structural elements in proteins (Jickells et al., 2005; Morel and Price, 2003; Shelley et al., 2015). Notably, Ni and V primarily originated from residual oil combustion, with contributions being markedly higher over the marine area (46.2–79.8%) compared to the coastal site (26.2–64.8%) (Fig.6d and e). However, the absolute concentrations of Ni and V from residual oil combustion were higher in the Qingdao atmosphere (Ni: 4.8–6.0 ng m⁻³, V: 12.8–16.2 ng m⁻³) than in the BS and YS atmosphere (Ni: 3.1–3.6 ng m⁻³, V: 8.2–9.6 ng m⁻³). This demonstrated that the emissions from residual oil combustion had a significant impact not only on the marine environment but, more notably, on the coastal urban air quality.

Over the BS and YS, coal combustion (21.3–41.2%), vehicular emissions (26.5–29.2%) and WI & IE (13.9–35.3%) contributed more significantly to Cu (Fig.6f). In Qingdao, WI & IE was an important source of Cu, consistent with observations in Beijing (Yang et al., 2022). Apart from the sea salt contributions, Zn originated from various anthropogenic sources including waste incineration, industrial emissions, coal combustion and secondary aerosol formation. In the marine area, coal combustion dominated Zn contributions, accounting for 31.5% and 52.5% of total Zn in spring and summer, respectively (Fig.6g).

470 4.3.3 Pb, Cd and As

Pb, Cd, and As, which are biologically toxic, pose potential non-carcinogenic or carcinogenic risks to human health and cause considerable detriment upon marine ecosystems (Nagajyoti et al., 2010; Zhang et al., 2018). Source apportionment revealed that coal combustion was the dominant contributor of Pb and Cd in **BS and YS** areas, particularly during summer, accounting for 71.6% of Pb and 78.8% of Cd (Fig.6h and i). The absolute concentrations revealed the land-to-sea transport: coal combustion contributed 4.6 ng m⁻³ of Pb to the marine atmosphere in summer, which was 1.8 times higher than its concentration in Qingdao (2.6 ng m⁻³), clearly indicating the pervasive influence of terrestrial coal emissions across the sea. In Beijing, the predominant sources of Pb were coal combustion in spring and industrial emissions in summer (Yang et al., 2022), mirroring our coastal observations. Similarly, coal combustion was identified as the primary source of As (34.6–75.0%), with its influence increasing over the **BS and YS** during spring (59.7%) and summer (75.0%) (Fig.6j). The emission inventory also indicates that 74.2% of As emissions can be ascribed to coal combustion in China (Tian et al., 2015). Furthermore, vehicular emissions also contributed significantly to As (12.3–56.6%), which can be attributed to the role of As as a recognized tracer for fossil fuel combustion (Chen et al., 2013). A interesting finding was the significant contribution of sea salt to Zn, Pb and Cd in marine environments during spring, indicating the mixing between SSAs and anthropogenic aerosols. The time series suggested that the peaks in sea salt contributions coincided with the high concentrations of Pb, Cd and Zn (Figs.4a and S3a), supporting that sea salt particles acted as a carrier for these toxic anthropogenic elements during transport.

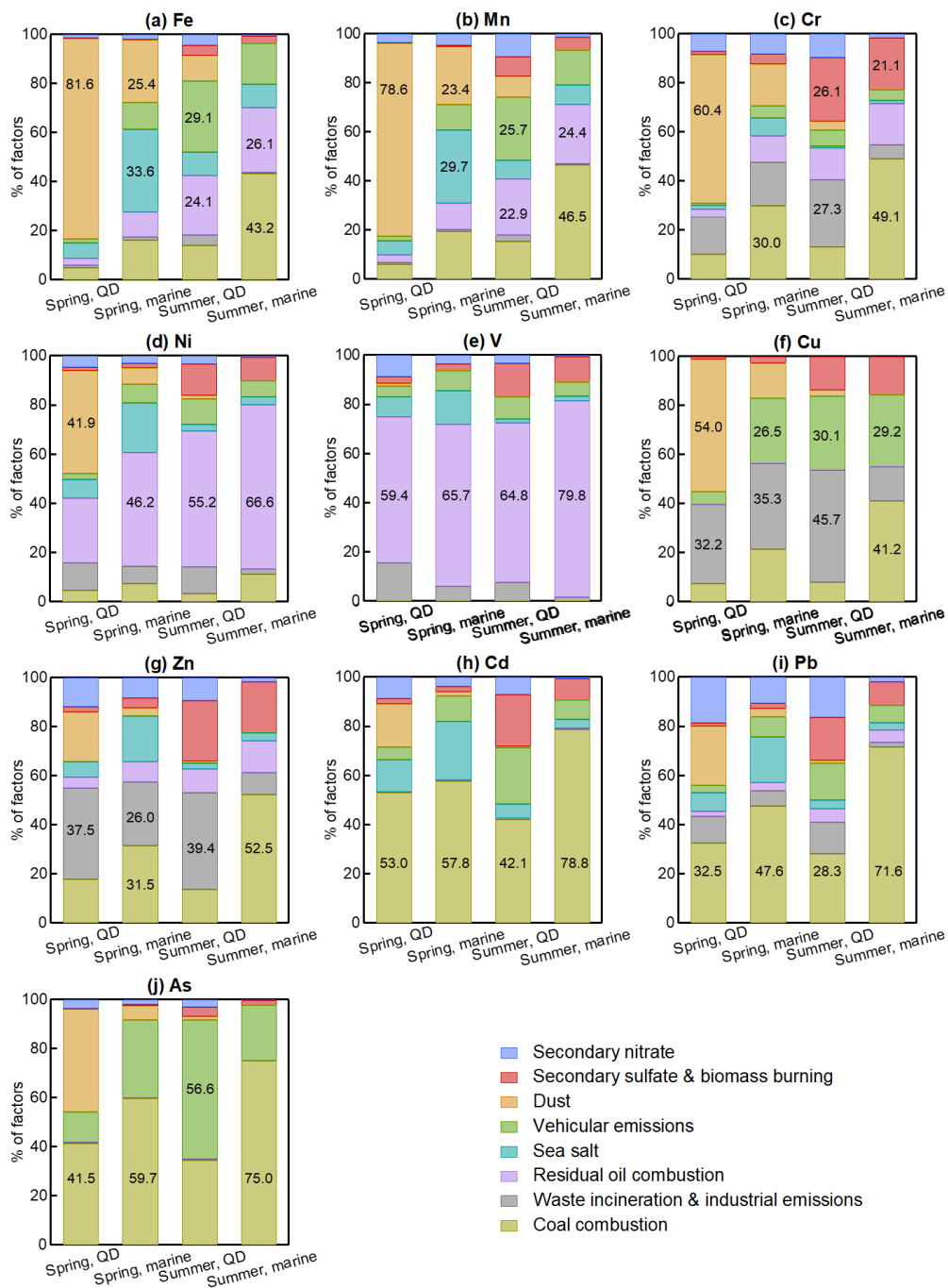


Figure 6: Percentage contributions of various source factors to individual elements based on PMF results. “marine” refers to the BS and YS.

5 Conclusions

490 This study investigated the spatial and seasonal distributions of $PM_{2.5}$ sources and associated trace elements in Qingdao and its adjacent offshore areas of the BS and YS during spring and summer 2018, delving into land-sea contrasts and the influence of anthropogenic activities on the marine air. Eight aerosol sources were identified in Qingdao and BS and YS regions, including secondary nitrate, the mixture of secondary sulfate and biomass burning, dust, vehicular emissions, sea salt, residual oil combustion (ship emissions), coal combustion, and the mixture of waste incineration and industrial pollutants.

495 Terrestrial-marine aerosol source gradients were driven by atmospheric transport and deposition processes. Secondary nitrate, primarily derived from terrestrial anthropogenic activities, exhibited a sharp land-to-sea decline, with contributions decreasing from 41.6% (Qingdao) to 23.6% (marine) in spring, and from 20.3% to 4.5% in summer. In contrast, secondary sulfate and biomass burning contributions increased slightly from Qingdao to marine areas: from 7.1% to 9.9% in spring, and from 46.1% to 51.0% in summer, reflecting enhanced sulfur precursor availability in marine areas and long-range transport over the marine

500 areas. Natural terrestrial sources (dust and dust-anthropogenic mixtures) demonstrated pronounced attenuation over marine areas due to size-dependent particle settling. For example, dust contributions declined from 19.6% (Qingdao) to 2.7% (marine) in spring. In contrast, finer anthropogenic particulates (e.g., vehicular emissions) exhibited enhanced offshore transport, with marine contributions (17.9%) exceeding those in Qingdao (6.9%) in spring. Summer southerly winds moderated this land-to-sea contrast. Marine-derived aerosols, particularly sea salt and ship emissions, dominated marine areas, with ship emissions

505 contributing up to 9.1% in spring and 14.7% in summer.

Trace element distributions mirrored aerosol source dynamics but with source-specific seasonal shifts. All TEs exhibited notably higher concentrations in Qingdao compared to marine in spring, where Zn, Pb, As, and Cd reversed this land-to-sea pattern in summer (marine > Qingdao), reflecting intensified anthropogenic influence over marine atmosphere. Regarding the sources distribution, traditional crustal TEs (Fe, Mn, Cr), terrestrial dust dominated their spring levels in Qingdao (Fe: 81.6%, 2832.0 $ng\ m^{-3}$; Mn: 78.6%, 92.7 $ng\ m^{-3}$; Cr: 60.4%, 6.9 $ng\ m^{-3}$), but contributions sharply decreased over marine areas (Fe: 25.4%, 145.2 $ng\ m^{-3}$; Mn: 23.4%, 4.8 $ng\ m^{-3}$; Cr: 16.9%, 0.4 $ng\ m^{-3}$). Instead, coal combustion became the dominant source of these elements, particularly in summer marine areas (Fe: 43.2%, 82.8 $ng\ m^{-3}$; Mn: 46.5%, 3.6 $ng\ m^{-3}$; Cr: 49.1%, 0.6 $ng\ m^{-3}$). Ship emissions not only dominated the Ni and V sources (except spring Qingdao Ni, 41.9% sourced from dust), but also contributed substantially to Fe, Mn and Cr, particularly in summer (Fe: 24.1%, 77.8 $ng\ m^{-3}$ in Qingdao and 26.1%, 50.0 $ng\ m^{-3}$ marine; Mn: 22.9%, 2.9 $ng\ m^{-3}$ in Qingdao and 24.4%, 1.9 $ng\ m^{-3}$ marine).

515 Springtime marine environments also showed elevated sea salt contributions to Fe, Mn, Zn, Cd, and Pb (18.5–33.6%), indicating extensive multi-source mixing (dust-sea salt-anthropogenic) in aerosols. The biogeochemical impact of this complex mixing on the reactivity of elements warrants further investigation.

These findings underscore the complex interplay of natural and anthropogenic drivers shaping coastal aerosol composition, and highlight the critical role of atmospheric transport and source-receptor dynamics as key controls on land-to-sea aerosol-borne element distributions and continental-marine aerosols interactions. They will further improve understanding of how

520

continental emissions influence offshore air quality and biogeochemical cycles, which is critical for refining regional air quality and climate models. Future work should investigate the reactivity of mixed-source aerosols to assess their environmental impacts (e.g. effects on TEs' solubility and modulation of marine productivity).

525

Data availability. The backward trajectories were calculated using the Hybrid Single-Particle Lagrangian Integrated Trajectory (HYSPLIT) transport model (<https://www.ready.noaa.gov/HYSPLIT.php>). The data associated with the figures in this manuscript, including Supporting Materials, are available in the in-text data citation reference Zhou (2025).

Author contribution.

530 **YQ:** formal analysis, writing-original draft, validation, writing-review & editing. **WL:** investigating, formal analysis, validation. **WQ:** methodology. **HZ:** methodology. **WZ:** investigating, formal analysis, validation. **JS:** writing-review & editing, methodology. **DZ:** validation, writing-review & editing. **YZ:** investigation, validation. **LS:** validation, writing-review. **WW:** validation, writing-review. **YZ:** investigation, validation. **YM:** investigation, validation. **DR:** investigation, validation. **GW:** investigation, validation. **XW:** methodology. **XY:** validation, methodology. **YZ:** conceptualization, writing-review & editing, validation, funding acquisition, supervision, project administration.

535

Competing interests. The authors declare that they have no conflict of interest.

Acknowledgments.

This research was sponsored by the National Natural Science Foundation of China (NSFC) (No. 42475119 and 41605114) and Shandong Provincial Natural Science Foundation (No. ZR2024MD016). The authors would like to thank all the colleagues who participated in these campaigns for their support. Data acquisition and sample collections were supported by NSFC Open Research Cruise (Cruise No. NORC2018-001), funded by Shiptime Sharing Project of NSFC. This cruise was conducted onboard R/V *DONGFANGHONG 2* by Ocean University of China. The authors gratefully acknowledge the NOAA-ARL for providing the HYSPLIT transport and dispersion model.

540

References

545 Adachi, K., Oshima, N., Gong, Z., de Sá, S., Bateman, A. P., Martin, S. T., de Brito, J. F., Artaxo, P., Cirino, G. G., Sedlacek III, A. J., and Buseck, P. R.: Mixing states of Amazon basin aerosol particles transported over long distances using transmission electron microscopy, *Atmos. Chem. Phys.*, 20, 11923-11939, <https://doi.org/10.5194/acp-20-11923-2020>, 2020.

- Amil, N., Latif, M. T., Khan, M. F., and Mohamad, M.: Seasonal variability of PM_{2.5} composition and sources in the Klang Valley urban-industrial environment, *Atmos. Chem. Phys.*, 16, 5357-5381, <https://doi.org/10.5194/acp-16-5357-2016>, 2016.
- 550 Andreae, M. O., Charlson, R. J., Bruynseels, F., Storms, H., Grieken, R. Van, and Maenhaut, W.: Internal mixture of sea salt, silicates, and excess sulfate in marine aerosols, *Science*, 232(4758), 1620-1623, <https://doi.org/10.1126/science.232.4758.1620>, 1986.
- Angle, K. J., Crocker, D. R., Simpson, R. M. C., Mayer, J. J., Garofalo, L. A., Moore, A. N., Mora Garcia, S. L., Or, V. W., Srinivasan, S., Farhan, M., Sauer, J. S., Lee, C., Pothier, M. A., Farmer, D. K., Martz, T. R., Bertram, T. H., Cappa, C. D.,
- 555 Prather, K. A., and Grassian, V. H.: Acidity across the interface from the ocean surface to sea spray aerosol, *P. Natl. Acad. Sci. USA*, 118, e2018397118, <https://doi.org/10.1073/pnas.2018397118>, 2021.
- Baker, A. R., and Jickells, T. D.: Mineral particle size as a control on aerosol iron solubility. *Geophys. Res. Lett.*, 33, L17608. <https://doi.org/10.1029/2006GL026557>, 2006.
- Baker, A. R., Jickells, T. D., Witt, M., and Linge, K. L.: Trends in the solubility of iron, aluminium, manganese and phosphorus
- 560 in aerosol collected over the Atlantic Ocean, *Mar. Chem.*, 98, 43-58, <https://doi.org/10.1016/j.marchem.2005.06.004>, 2006.
- Bie, S., Yang, L., Zhang, Y., Huang, Q., Li, J., Zhao, T., Zhang, X., Wang, P., and Wang, W.: Source appointment of PM_{2.5} in Qingdao Port, East of China, *Sci. Total. Environ.*, 755, <https://doi.org/10.1016/j.scitotenv.2020.142456>, 2021.
- Borai, E. H., El-Sofany, E. A., Abdel-Halim, A. S., and Soliman, A. A.: Speciation of hexavalent chromium in atmospheric particulate samples by selective extraction and ion chromatographic determination, *Trac-Trend. Anal. Chem.*, 21, 741-745,
- 565 [https://doi.org/10.1016/S0165-9936\(02\)01102-0](https://doi.org/10.1016/S0165-9936(02)01102-0), 2002.
- Boyd, P. W., Watson, A. J., Law, C. S., Abraham, E. R., Trull, T., Murdoch, R., Bakker, D. C. E., Bowie, A. R., Buesseler, K. O., Chang, H., Charette, M., Croot, P., Downing, K., Frew, R., Gall, M., Hadfield, M., Hall, J., Harvey, M., Jameson, G., LaRoche, J., Liddicoat, M., Ling, R., Maldonado, M. T., McKay, R. M., Nodder, S., Pickmere, S., Pridmore, R., Rintoul, S., Safi, K., Sutton, P., Strzeppek, R., Tanneberger, K., Turner, S., Waite, A., and Zeldis, J.: A mesoscale phytoplankton bloom in
- 570 the polar Southern Ocean stimulated by iron fertilization, *Nature*, 407, 695-702, <https://doi.org/10.1038/35037500>, 2000.
- Buck, C. S., Landing, W. M., and Resing, J. A.: Particle size and aerosol iron solubility: A high-resolution analysis of Atlantic aerosols, *Mar. Chem.*, 120, 14-24, <https://doi.org/10.1016/j.marchem.2008.11.002>, 2010.
- Chang, Y., Huang, K., Xie, M., Deng, C., Zou, Z., Liu, S., and Zhang, Y.: First long-term and near real-time measurement of trace elements in China's urban atmosphere: Temporal variability, source apportionment and precipitation effect. *Atmos. Chem. Phys.*, 18, 11793-11812. <https://doi.org/10.5194/acp-18-11793-2018>, 2018.
- Chen, J., Liu, G., Kang, Y., Wu, B., Sun, R. Y., Zhou, C. C., and Wu., D.: Atmospheric emissions of F, As, Se, Hg, and Sb from coal-fired power and heat generation in China, *Chemosphere*, 90, 1925-1932, <http://doi.org/10.1016/j.chemosphere.2012.10.032>, 2013.
- Chen, J., Tan, M., Li, Y., Zheng, J., Zhang, Y., Shan, Z., Zhang, G., and Li, Y.: Characteristics of trace elements and lead
- 580 isotope ratios in PM_{2.5} from four sites in Shanghai, *J. Hazard. Mater.*, 156, 36-43, <https://doi.org/10.1016/j.jhazmat.2007.11.122>, 2008.

- Choobari, O. A., Zawar-Reza, P., and Sturman, A.: The global distribution of mineral dust and its impacts on the climate system: A review, *Atmos. Res.*, 138, 152-165, <https://doi.org/10.1016/j.atmosres.2013.11.007>, 2014.
- Draxler, R. R., and Rolph, G. D.: HYSPLIT (HYbrid Single-Particle Lagrangian Integrated Trajectory) Model access via
585 NOAA ARL READY Website, last, NOAA Air Resources Laboratory, College Park, MD, 2014.
- Desboeufs, K. V., Losno, R., Vimeux, F., and Cholbi, S.: The pH - dependent dissolution of wind - transported Saharan dust, *J. Geophys. Res.*, 104, 21,287–21,299, <https://doi.org/10.1029/1999JD900236>, 1999.
- Falkowski, P. G., Barber, R. T., and Smetacek, V.: Biogeochemical controls and feedbacks on ocean primary production, *Science*, 281, 200-206, <https://doi.org/10.1126/science.281.5374.200>, 1998.
- 590 Feng, L., Shen, H., Zhu, Y., Gao, H., and Yao, X.: Insight into Generation and Evolution of Sea-Salt Aerosols from Field Measurements in Diversified Marine and Coastal Atmospheres, *Sci. Rep.*, 7, 41260, <https://doi.org/10.1038/srep41260>, 2017.
- Gen, M., Zhang, R., and Chen, C. K.: Nitrite/Nitrous Acid Generation from the Reaction of Nitrate and Fe(II) Promoted by Photolysis of Iron-Organic Complexes. *Environ. Sci. Technol.*, 55, 15715-15723. <https://doi.org/10.1021/acs.est.1c05641>, 2022.
- 595 Geng, H., Hwang, H., Liu, X., Dong, S., and Ro, C. U.: Investigation of aged aerosols in size-resolved Asian dust storm particles transported from Beijing, China, to Incheon, Korea, using low-Z particle EPMA. *Atmos. Chem. Phys.*, 14, 3307-3323. <https://doi.org/10.5194/acp-14-3307-2014>. 2014.
- Gu, J., Pitz, M., Schnelle-Kreis, J., Diemer, J., Reller, A., Zimmermann, R., Soentgen, J., Stoelzel, M., Wichmann, H.-E., Peters, A., and Cyrys, J.: Source apportionment of ambient particles: Comparison of positive matrix factorization analysis
600 applied to particle size distribution and chemical composition data, *Atmos. Environ.*, 45, 1849-1857, <https://doi.org/10.1016/j.atmosenv.2011.01.009>, 2011.
- Gugamsetty, B., Wei, H., Liu, C. N., Awasthi, A., Hsu, S. C., Tsai, C. J., Roam, G. D., Wu, Y. C., and Chen, C. F.: Source Characterization and Apportionment of PM₁₀, PM_{2.5} and PM_{0.1} by Using Positive Matrix Factorization, *Aerosol Air Qual. Res.*, 12, 476-491, <https://doi.org/10.4209/aaqr.2012.04.0084>, 2012.
- 605 Hawco, N. J., Tagliabue, A. and Twining, B. S.: Manganese limitation of phytoplankton physiology and productivity in the Southern Ocean. *Global Biogeochem. Cycles*, 36, e2022GB007382. <https://doi.org/10.1029/2022GB007382>, 2022.
- Hilario, M. R. A., Cruz, M. T., Cambaliza, M. O. L., Reid, J. S., Xian, P., Simpas, J. B., Lagrosas, N. D., Uy, S. N. Y., Cliff, S., and Zhao, Y.: Investigating size-segregated sources of elemental composition of particulate matter in the South China Sea during the 2011 Vasco cruise, *Atmos. Chem. Phys.*, 20, 1255-1276, <https://doi.org/10.5194/acp-20-1255-2020>, 2020.
- 610 Ho, K. F., Lee, S. C., Chow, J. C., and Watson, J. G.: Characterization of PM₁₀ and PM_{2.5} source profiles for fugitive dust in Hong Kong, *Atmos. Environ.*, 37, 1023-1032, [https://doi.org/10.1016/S1352-2310\(02\)01028-2](https://doi.org/10.1016/S1352-2310(02)01028-2), 2003.
- Hsieh, C. -C., Chen, H. -Y., & Ho, T. -Y.: The effect of aerosol size on Fe solubility and deposition flux: A case study in the East China Sea, *Mar. Chem.*, 241, 104106, <https://doi.org/10.1016/j.marchem.2022.104106>, 2022.
- Hsieh, C. -C., You, C. -F., & Ho, T. -Y.: The solubility and deposition flux of East Asian aerosol metals in the East China Sea: The effects of aeolian transport processes, *Mar. Chem.*, 253, 104268, <https://doi.org/10.1016/j.marchem.2023.104268>, 2023.
- 615

- Hsu, S.-C., Liu, S. C., Arimoto, R., Shiah, F.-K., Gong, G.-C., Huang, Y.-T., Kao, S.-J., Chen, J.-P., Lin, F.-J., Lin, C.-Y., Huang, J.-C., Tsai, F., and Lung, S.-C. C.: Effects of acidic processing, transport history, and dust and sea salt loadings on the dissolution of iron from Asian dust, *J. Geophys. Res.-Atmos.*, 115, D19313. <https://doi.org/10.1029/2009JD013442>, 2010.
- 620 Hsu, S. C., Wong, G. T. F., Gong, G. C., Shiah, F. K., Huang, Y. T., Kao, S. J., Tsai, F. J., Lung, S. C. C., Lin, F. J., Lin, H., Hung, C. C., and Tseng, C. M.: Sources, solubility, and dry deposition of aerosol trace elements over the East China Sea, *Mar. Chem.*, 120, 116-127, <https://doi.org/10.1016/j.marchem.2008.10.003>, 2010.
- Hsu, S. -C., Liu, S. C., Kao, S. J., Jeng, W. L., Huang, Y. T., Tseng, C. M., Tsai, F., Tu, J. Y., and Yang, T.: Water - soluble species in the marine aerosol from the northern South China Sea: High chloride depletion related to air pollution, *J. Geophys. Res.*, 112, D19304, <https://doi.org/10.1029/2007JD008844>, 2007.
- 625 Huang, J., Wang, T., Wang, W., Li, Z., and Yan, H.: Climate effects of dust aerosols over East Asian arid and semiarid regions, *J. Geophys. Res.-Atmos.*, 119, 11398-11416, <https://doi.org/10.1002/2014JD021796>, 2014.
- Ito, A. and Feng, Y.: Iron mobilization in North African Dust, *Earth System Science 2010: Global Change, Climate and People*, WOS:000312268000004, <https://doi.org/10.1016/j.proenv.2011.05.004>, 2011.
- Ito, A., Ye, Y., Baldo, C., and Shi, Z. B.: Ocean fertilization by pyrogenic aerosol iron. *npj Clim. Atmos. Sci.*, 4, Article 30. <https://doi.org/10.1038/s41612-021-00185-8>, 2021.
- 630 Jickells, T. D., An, Z. S., Andersen, K. K., Baker, A. R., Bergametti, G., Brooks, N., Cao, J. J., Boyd, P. W., Duce, R. A., Hunter, K. A., Kawahata, H., Kubilay, N., laRoche, J., Liss, P. S., Mahowald, N., Prospero, J. M., Ridgwell, A. J., Tegen, I., and Torres, R.: Global iron connections between desert dust, ocean biogeochemistry, and climate, *Science*, 308, 67-71, <https://doi.org/10.1126/science.1105959>, 2005.
- 635 Karar, K., Gupta, A. K., Kumar, A., and Biswas, A. K.: Characterization and identification of the sources of chromium, zinc, lead, cadmium, nickel, manganese and iron in Pm-10 particulates at the two sites of kolkata, india, *Environ. Monit. Assess.*, 120, 347-360, <https://doi.org/10.1007/s10661-005-9067-7>, 2006.
- Kim, N., Yum, S. S., Cho, S., Jung, J., Lee, G., and Kim, H.: Atmospheric sulfate formation in the Seoul Metropolitan Area during spring/summer: Effect of trace metal ions. *Environ. Pollut.*, 315, 120379. <https://doi.org/10.1016/j.envpol.2022.120379>,
- 640 2022.
- Knopf, D. A., Charnawskas, J. C., Wang, P., Wong, B., Tomlin, J. M., Jankowski, K. A., Fraund, M., Veghte, D. P., China, S., Laskin, A., Moffet, R. C., Gilles, M. K., Aller, J. Y., Marcus, M. A., Raveh-Rubin, S., and Wang, J.: Micro-spectroscopic and freezing characterization of ice-nucleating particles collected in the marine boundary layer in the eastern North Atlantic, *Atmos. Chem. Phys.*, 22, 5377–5398, <https://doi.org/10.5194/acp-22-5377-2022>, 2022.
- 645 Kwak, N., Lee, H., Maeng, H., Seo, A., Lee, K., Kim, S., Lee, M., Cha, J. W., Shin, B., and Park, K.: Morphological and chemical classification of fine particles over the Yellow Sea during spring, 2015–2018, *Environ. Pollut.*, 305, 119286, <https://doi.org/10.1016/j.envpol.2022.119286>, 2022.
- Lee, J. H., Hopke, P. K., and Turner, J. R.: Source identification of airborne PM_{2.5} at the St. Louis-Midwest Supersite, *J. Geophys. Res.-Atmos.*, 111, <https://doi.org/10.1029/2005JD006329>, 2006.

- 650 Li, P., Li, Q., Shi, J., Gao, H., and Yao, X.: Concentration, solubility, and dry deposition flux of trace elements in fine and coarse particles in Qingdao during summer (in Chinese), *Environ. Sci.*, 39, 3067-3074, <https://doi.org/10.13227/j.hjcx.201712231>, 2018.
- Li, Q., Cheng, H., Zhou, T., Lin, C., and Guo, S.: The estimated atmospheric lead emissions in China, 1990-2009, *Atmos. Environ.*, 60, 1-8, <https://doi.org/10.1016/j.atmosenv.2012.06.025>, 2012.
- 655 Li, R., Wang, Q., He, X., Zhu, S., Zhang, K., Duan, Y., Fu, Q., Qiao, L., Wang, Y., Huang, L., Li, L., and Yu, J. Z.: Source apportionment of PM_{2.5} in Shanghai based on hourly organic molecular markers and other source tracers, *Atmos. Chem. Phys.*, 20, 12047-12061, <https://doi.org/10.5194/acp-20-12047-2020>, 2020.
- Li, T., Wang, Y., Li, W., Chen, J., Wang, T., and Wang, W.: Concentrations and solubility of trace elements in fine particles at a mountain site, southern China: regional sources and cloud processing, *Atmos. Chem. Phys.*, 15, 8987-9002, <https://doi.org/10.5194/acp-15-8987-2015>, 2015.
- 660 Li, T., Wang, Y., Zhou, J., Wang, T., Ding, A., Nie, W., Xue, L., Wang, X., and Wang, W.: Evolution of trace elements in the planetary boundary layer in southern China: Effects of dust storms and aerosol-cloud interactions, *J. Geophys. Res.-Atmos.*, 122, 3492-3506, <https://doi.org/10.1002/2016JD025541>, 2017.
- Li, W., Qi, Y., Liu, Y., Wu, G., Zhang, Y., Shi, J., Qu, W., Sheng, L., Wang, W., Zhang, D., and Zhou, Y.: Daytime and nighttime aerosol soluble iron formation in clean and slightly polluted moist air in a coastal city in eastern China. *Atmos. Chem. Phys.*, 24, 6495-6508. <https://doi.org/10.5194/acp-24-6495-2024>, 2024.
- 665 Li, W., Qi, Y., Qu, W., Qu, W., Shi, J., Zhang, D., Liu, Y., Wu, F., Ma, Y., Zhang, Y., Ren, D., Du, X., Yang, S., Wang, X., Yi, L., Gao, X., Wang, W., Ma, Y., Sheng, L., and Zhou, Y.: Sulfate and nitrate elevation in reverse-transport dust plumes over coastal areas of China. *Atmos. Environ.*, 295, 119518, Article 119518. <https://doi.org/10.1016/j.atmosenv.2022.119518>, 2023.
- 670 Li, W., Wang, W., Zhou, Y., Ma, Y., Zhang, D., and Sheng, L.: Occurrence and Reverse Transport of Severe Dust Storms Associated with Synoptic Weather in East Asia, *Atmosphere*, 10, <https://doi.org/10.3390/atmos10010004>, 2019.
- Li, Y.-X., Luo, L., Li, J.-W., Hsu, S.-C, Ni, Y.-Z., and Kao, S.-J.: Middle East and Central Asian dust reaches the South China Sea in summer. *Natl. Sci. Rev.*, nwaf274. <https://doi.org/10.1093/nsr/nwaf274>, 2025.
- 675 Li, Z., Ho, K.-F., Dong, G., Lee, H. F., and Yim, S. H. L.: A novel approach for assessing the spatiotemporal trend of health risk from ambient particulate matter components: Case of Hong Kong. *Environ. Res.*, 204, 111866. <https://doi.org/10.1016/j.envres.2021.111866>, 2022.
- Lin, Y.-C., Yu, M., Xie, F., and Zhang, Y. Anthropogenic Emission Sources of Sulfate Aerosols in Hangzhou, East China: Insights from Isotope Techniques with Consideration of Fractionation Effects between Gas-to-Particle Transformations. *Environ. Sci. Technol.*, 56, 3905-3914. <https://doi.org/10.1021/acs.est.1c05823>, 2022.
- 680 Liu, B., Song, N., Dai, Q., Mei, R., Sui, B., Bi, X., and Feng, Y.: Chemical composition and source apportionment of ambient PM_{2.5} during the non-heating period in Taian, China, *Atmos. Res.*, 170, 23-33, <https://doi.org/10.1016/j.atmosres.2015.11.002>, 2016.

- Liu, B., Sun, X., Zhang, J., Bi, X., Li, Y., Li, L., Dong, H., Xiao, Z., Zhang, Y., and Feng, Y.: Characterization and Spatial
685 Source Apportionments of Ambient PM₁₀ and PM_{2.5} during the Heating Period in Tian'jin, China, *Aerosol Air Qual. Res.*,
20, 1-13, <https://doi.org/10.4209/aaqr.2019.06.0281>, 2020.
- López-García, P., Gelado-Caballero, M. D., Collado-Sánchez, C., and Hernández-Brito, J. J.: Solubility of aerosol trace
elements: Sources and deposition fluxes in the Canary Region, *Atmos. Environ.*, 148, 167-174,
<https://doi.org/10.1016/j.atmosenv.2016.10.035>, 2017.
- 690 Luo, C., Mahowald, N., Bond, T., Chuang, P. Y., Artaxo, P., Siefert, R., Chen, Y., and Schauer, J.: Combustion iron distribution
and deposition, *Global Biogeochem. Cy.*, 22, <https://doi.org/10.1029/2007GB002964>, 2008.
- Luo, C. H., Wang, W. C., Sheng, L. F., Zhou, Y., Hu, Z. Y., Qu, W. J., Li, X. D., and Hai, S. F.: Influence of polluted dust on
chlorophyll-a concentration and particulate organic carbon in the subarctic North Pacific Ocean based on satellite observation
and the WRF-Chem simulation, *Atmos. Res.*, 236, 104812, <https://doi.org/10.1016/j.atmosres.2019.104812>, 2020.
- 695 Ma, Y. N., Ma, Y. J., Zhang, X. G., Wu, F. K., Liu, Q., Wu, X. Y., Lyu, Y., Jiang, J. W., Zhao, D. D., Ren, X. B., Li, Z., Jia,
X., Li, M. C., Yao, J. Y., Gao, Z. M., Hai, S. F., and Xin, J. Y. Shipboard Observations of Aerosol Chemical Properties Over
the Western Pacific Ocean in Winter 2018. *J. Geophys. Res.-Atmos.*, 128, Article e2023JD039422.
<https://doi.org/10.1029/2023JD039422>, 2023.
- Mahowald, N.: Aerosol Indirect Effect on Biogeochemical Cycles and Climate, *Science*, 334, 794-796,
700 <https://doi.org/10.1126/science.1207374>, 2011.
- Mann, E. L., Ahlgren, N., Moffett, J. W., and Chisholm, S. W.: Copper toxicity and cyanobacteria ecology in the Sargasso
Sea, *Limnol. Oceanogr.*, 47, 976-988, <https://doi.org/10.4319/lo.2002.47.4.0976>, 2002.
- Martin, J. H.: Glacial-interglacial CO₂ change: The iron hypothesis, *Paleoceanography*, 5, 1-13,
<https://doi.org/10.1029/PA005i001p00001>, 1990.
- 705 Meng, Y., Li, P., Cao, W., Shi, J., Gao, H., and Yao, X.: Size distribution of particulate trace elements in mass concentration
and their size-dependent solubility in the atmosphere in Qingdao, China (in Chinese), *China Environ. Sci.*, 37, 851-858, 2017.
- Ming, L., Jin, L., Li, J., Fu, P., Yang, W., Liu, D., Zhang, G., Wang, Z., and Li, X.: PM_{2.5} in the Yangtze River Delta, China:
Chemical compositions, seasonal variations, and regional pollution events. *Environ. Pollut.*, 223, 200-212.
<https://doi.org/10.1016/j.envpol.2017.01.013>, 2017.
- 710 Morel, F. M. M. and Price, N. M.: The biogeochemical cycles of trace metals in the oceans, *Science*, 300, 944-947,
<https://doi.org/10.1126/science.1083545>, 2003.
- Mustaffa, N. I. H., Latif, M. T., Ali, M. M., and Khan, M. F.: Source apportionment of surfactants in marine aerosols at
different locations along the Malacca Straits, *Environ. Sci. Pollut. R.*, 21, 6590-6602, <https://doi.org/10.1007/s11356-014-2562-z>, 2014.
- 715 Nagajyoti, P. C., Lee, K. D., and Sreekanth, T. V. M.: Heavy metals, occurrence and toxicity for plants: a review. *Environ.*
Chem. Lett., 8, 199-216. <https://doi.org/10.1007/s10311-010-0297-8>, 2010.

- Norris, G., Duvall, R., Brown, S., and Bai, S.: EPA positive matrix factorization (PMF) 5.0 fundamentals and user guide, US Environmental Protection Agency Office of Research and Development, Washington, DC, <https://www.epa.gov/air-research/epa-positive-matrix-factorization-50-fundamentals-and-user-guide>, 2014.
- 720 Okada, K., Naruse, H., Tanaka, T., Nemoto, O., Iwasaka, Y., Wu, P. -M., Ono, A., Duce, R. A., Uematsu, M., Merrill, J. T., and Arao, K.: X-ray spectrometry of individual Asian dust-storm particles over the Japanese islands and the North Pacific Ocean, *Atmos. Environ.*, 24(6), 1369-1378, [https://doi.org/10.1016/0960-1686\(90\)90043-M](https://doi.org/10.1016/0960-1686(90)90043-M), 1990.
- Paatero, P. and Tapper, U.: Positive matrix factorization - a nonnegative factor model with optimal utilization of error-estimates of data values, *Environmetrics*, 5, 111-126, <https://doi.org/10.1002/env.3170050203>, 1994.
- 725 Pant, P. and Harrison, R. M.: Estimation of the contribution of road traffic emissions to particulate matter concentrations from field measurements: A review, *Atmos. Environ.*, 77, 78-97, <https://doi.org/10.1016/j.atmosenv.2013.04.028>, 2013.
- Peng, L., Cui, X., Wang, X., Guo, Y., Ma, Y., Wen, Y., Wang, Z., Guo, Y., and Sun, J. Occurrence, source, and ecological impacts of dry depositing aerosol metal elements in the Bohai Bay. *Mar. Environ. Res.*, 208, 107137. <https://doi.org/10.1016/j.marenvres.2025.107137>, 2025.
- 730 Polissar, A. V., Hopke, P. K., and Poirot, R. L.: Atmospheric aerosol over Vermont: Chemical composition and sources, *Environ. Sci. Technol.*, 35, 4604-4621, <https://doi.org/10.1021/es0105865>, 2001.
- Prijith, S. S., Aloysius, M., and Mohan, M.: Relationship between wind speed and sea salt aerosol production: A new approach, *J. Atmos. Sol.-Terr. Phys.*, 108, 34-40, <https://doi.org/10.1016/j.jastp.2013.12.009>, 2014.
- Qi, Y. and Zhou, Y.: A review of the iron and its solubility in atmospheric aerosols (in Chinese), *J. Mar. Meteorol.*, 41, 1-13, <https://doi.org/10.19513/j.cnki.issn2096-3599.2021.02.001>, 2021.
- 735 Qiu, S.: Solubility of iron in atmospheric aerosols and related factors in Marginal Seas, China (in Chinese), M.S. Thesis, Ocean University of China, Qingdao, China, 2015.
- Rai, P., Chakraborty, A., Mandariya, A. K., and Gupta, T.: Composition and source apportionment of PM1 at urban site Kanpur in India using PMF coupled with CBPF, *Atmos. Res.*, 178, 506-520, <https://doi.org/10.1016/j.atmosres.2016.04.015>, 2016.
- 740 Ramanathan, V., Ramana, M. V., Roberts, G., Kim, D., Corrigan, C., Chung, C., and Winker, D.: Warming trends in Asia amplified by brown cloud solar absorption, *Nature*, 448, 575-U575, <https://doi.org/10.1038/nature06019>, 2007.
- Sakata, K., Kurisu, M., Takeichi, Y., Sakaguchi, A., Tanimoto, H., Tamenori, Y., Matsuki, A., and Takahashi, Y.: Iron (Fe) speciation in size-fractionated aerosol particles in the Pacific Ocean: The role of organic complexation of Fe with humic-like substances in controlling Fe solubility, *Atmos. Chem. Phys.*, 22, 9461-9482, <https://doi.org/10.5194/acp-22-9461-2022>, 2022.
- 745 Schroth, A. W., Crusius, J., Sholkovitz, E. R., and Bostick, B. C.: Iron solubility driven by speciation in dust sources to the ocean, *Nat. Geosci.*, 2, 337-340, <https://doi.org/10.1038/NGEO501>, 2009.
- Sharma, S. K., Sharma, A., Saxena, M., Choudhary, N., Masiwal, R., Mandal, T. K., and Sharma, C.: Chemical characterization and source apportionment of aerosol at an urban area of Central Delhi, India, *Atmos. Pollut. Res.*, 7, 110-121, <https://doi.org/10.1016/j.apr.2015.08.002>, 2016.

- 750 Shelley, R. U., Morton, P. L., and Landing, W. M.: Elemental ratios and enrichment factors in aerosols from the US-GEOTRACES North Atlantic transects, *Deep-Sea Res. Pt. II*, 116, 262-272, <https://doi.org/10.1016/j.dsr2.2014.12.005>, 2015.
- Shi, J.-H., Zhang, J., Gao, H.-W., Tan, S.-C., Yao, X.-H., and Ren, J.-L.: Concentration, solubility and deposition flux of atmospheric particulate nutrients over the Yellow Sea, *Deep-Sea Res. Pt. II*, 97, 43-50, <https://doi.org/10.1016/j.dsr2.2013.05.004>, 2013.
- 755 Shi, Z., Krom, M. D., Jickells, T. D., Bonneville, S., Carslaw, K. S., Mihalopoulos, N., Baker, A. R., and Benning, L. G.: Impacts on iron solubility in the mineral dust by processes in the source region and the atmosphere: A review, *Aeolian Res.*, 5, 21-42, <https://doi.org/10.1016/j.aeolia.2012.03.001>, 2012.
- Sholkovitz, E. R., Sedwick, P. N., Church, T. M., Baker, A. R., and Powell, C. F.: Fractional solubility of aerosol iron: Synthesis of a global-scale data set, *Geochim. Cosmochim. Ac.*, 89, 173-189, <https://doi.org/10.1016/j.gca.2012.04.022>, 2012.
- 760 Sorooshian, A., Wang, Z., Coggon, M. M., Jonsson, H. H., and Ervens, B.: Observations of Sharp Oxalate Reductions in Stratocumulus Clouds at Variable Altitudes: Organic Acid and Metal Measurements During the 2011 E-PEACE Campaign, *Environ. Sci. Technol.*, 47, 7747-7756, <https://doi.org/10.1021/es4012383>, 2013.
- Spokes, L. J., and Jickells, T. D.: Factors controlling the solubility of aerosol trace metals in the atmosphere and on mixing into seawater, *Aquat. Geochem.*, 1, 355-374, <https://doi.org/10.1007/BF00702739>, 1996.
- 765 Sun, H., Sun, J., Zhu, C., Yu, L., Lou, Y., Li, R., and Lin, Z.: Chemical characterizations and sources of PM2.5 over the offshore Eastern China sea: Water soluble ions, stable isotopic compositions, and metal elements. *Atmos. Pollut. Res.*, 13, 101410. <https://doi.org/10.1016/j.apr.2022.101410>, 2022.
- Sun, M., Qi, Y., Li, W., Zhu, W., Yang, Y., Wu, G., Zhang, Y., Zhao, Y., Shi, J., Sheng, L., Wang, W., Liu, Y., Qu, W., Wang, X., and Zhou, Y. Investigation of a haze-to-dust and dust swing process at a coastal city in northern China part II: A study on the solubility of iron and manganese across aerosol sources and secondary processes. *Atmos. Environ.*, 328, 120532. <https://doi.org/10.1016/j.atmosenv.2024.120532>, 2024.
- Tang, W. Y., Llorc, J., Weis, J., Perron, M. M. G., Basart, S., Li, Z. C., Sathyendranath, S., Jackson, T., Rodriguez, E. S., Proemse, B. C., Bowie, A. R., Schallenberg, C., Strutton, P. G., Matear, R., and Cassar, N.: Widespread phytoplankton blooms triggered by 2019-2020 Australian wildfires, *Nature*, 597, 370-375, <https://doi.org/10.1038/s41586-021-03805-8>, 2021.
- 775 Taylor, S. R.: Trace element abundances and the chondritic earth model, *Geochim. Cosmochim. Ac.*, 28, 1989-1998, [https://doi.org/10.1016/0016-7037\(64\)90142-5](https://doi.org/10.1016/0016-7037(64)90142-5), 1964.
- Tian, H., Cheng, K., Wang, Y., Zhao, D., Lu, L., Jia, W., and Hao, J.: Temporal and spatial variation characteristics of atmospheric emissions of Cd, Cr, and Pb from coal in China, *Atmos. Environ.*, 50, 157-163, <https://doi.org/10.1016/j.atmosenv.2011.12.045>, 2012.
- 780 Tian, H., Liu, K., Zhou, J., Lu, L., Hao, J., Qiu, P., Gao, J., Zhu, C., Wang, K., and Hua, S.: Atmospheric Emission Inventory of Hazardous Trace Elements from China's Coal-Fired Power Plants-Temporal Trends and Spatial Variation Characteristics, *Environ. Sci. Technol.*, 48, 3575-3582, <http://doi.org/10.1021/es404730j>, 2014.

- Vu, T. V., Delgado-Saborit, J. M., and Harrison, R. M.: Review: Particle number size distributions from seven major sources and implications for source apportionment studies, *Atmos. Environ.*, 122, 114-132, 785 <https://doi.org/10.1016/j.atmosenv.2015.09.027>, 2015.
- Wagener, T., Guieu, C., Losno, R., Bonnet, S., and Mahowald, N.: Revisiting atmospheric dust export to the Southern Hemisphere ocean: Biogeochemical implications, *Global Biogeochem. Cycles*, 22, GB2006, <https://doi.org/10.1029/2007GB002984>, 2008.
- Wang, L., Qi, J. H., Shi, J. H., Chen, X. J., and Gao, H. W.: Source apportionment of particulate pollutants in the atmosphere 790 over the Northern Yellow Sea, *Atmos. Environ.*, 70, 425-434, <https://doi.org/10.1016/j.atmosenv.2012.12.041>, 2013.
- Wang, Q., Qiao, L., Zhou, M., Zhu, S., Griffith, S., Li, L., and Yu, J. Z.: Source Apportionment of PM_{2.5} Using Hourly Measurements of Elemental Tracers and Major Constituents in an Urban Environment: Investigation of Time-Resolution Influence, *J. Geophys. Res.-Atmos.*, 123, 5284-5300, <https://doi.org/10.1029/2017JD027877>, 2018.
- Wang, W., Luo, C., Sheng, L., Zhao, C., Zhou, Y., and Chen, Y.: Effects of biomass burning on chlorophyll-a concentration 795 and particulate organic carbon in the subarctic North Pacific Ocean based on satellite observations and WRF-Chem model simulations: A case study, *Atmos. Res.*, 254, 105526, <https://doi.org/10.1016/j.atmosres.2021.105526>, 2021.
- Wang, W. C., He, Z. Z., Hai, S. F., Sheng, L. F., Han, Y. Q., and Zhou, Y.: Dust Aerosol's Deposition and its Effects on Chlorophyll-A Concentrations Based on Multi-Sensor Satellite Observations and Model Simulations: A Case Study, *Front. Env. Sci.-Switz.*, 10, 875365, <https://doi.org/10.3389/fenvs.2022.875365>, 2022.
- 800 Wang, Y., Cheng, K., Tian, H.-Z., Yi, P., and Xue, Z.-G.: Emission Characteristics and Control Prospects of Primary PM_{2.5} from Fossil Fuel Power Plants in China, *Aerosol Air Qual. Res.*, 16, 3290-3301, <http://doi.org/10.4209/aaqr.2016.07.0324>, 2016.
- Wu, C., Huang, X. H. H., Ng, W. M., Griffith, S. M., and Yu, J. Z.: Inter-comparison of NIOSH and IMPROVE protocols for OC and EC determination: implications for inter-protocol data conversion, *Atmos. Meas. Tech.*, 9, 4547-4560, 805 <https://doi.org/10.5194/amt-9-4547-2016>, 2016.
- Wu, H. Y., Hsieh, C. C., and Ho, T. Y.: Trace metal dissolution kinetics of East Asian size-fractionated aerosols in seawater: The effect of a model siderophore, *Mar. Chem.*, 254, 104277, <https://doi.org/10.1016/j.marchem.2023.104277>, 2023.
- Wu, R., Zhou, X., Wang, L., Wang, Z., Zhou, Y., Zhang, J., and Wang, W.: PM_{2.5} Characteristics in Qingdao and across Coastal Cities in China, *Atmosphere*, 8, <https://doi.org/10.3390/atmos8040077>, 2017.
- 810 Wu, S. P., Cai, M. J., Xu, C., Zhang, N., Zhou, J. B., Yan, J. P., Schwab, J. J., and Yuan, C. S.: Chemical nature of PM_{2.5} and PM₁₀ in the coastal urban Xiamen, China: Insights into the impacts of shipping emissions and health risk, *Atmos. Environ.*, 227, <https://doi.org/10.1016/j.atmosenv.2020.117383>, 2020.
- Xu, B., Xu, H., Zhao, H., Gao, J., Liang, D., Li, Y., Wang, W., Feng, Y., and Shi, G.: Source apportionment of fine particulate matter at a megacity in China, using an improved regularization supervised PMF model. *Sci. Total Environ.*, 879, 163198. 815 <https://doi.org/10.1016/j.scitotenv.2023.163198>, 2023.

- Xu, L., Liu, X. H., Gao, H. W., Yao, X. H., Zhang, D. Z., Bi, L., Liu, L., Zhang, J., Zhang, Y. X., Wang, Y. Y., Yuan, Q., and Li, W. J.: Long-range transport of anthropogenic air pollutants into the marine air: insight into fine particle transport and chloride depletion on sea salts. *Atmos. Chem. Phys.*, 21, 17715-17726. <https://doi.org/10.5194/acp-21-17715-2021>, 2021.
- Xu, L., Zhi, M. K., Liu, X. H., Gao, H. W., Yao, X. H., Yuan, Q., Fu, P. Q., and Li, W. J.: Direct evidence of pyrogenic aerosol iron by intrusions of continental polluted air into the Eastern China Seas, *Atmos. Res.*, 292, 106839, <https://doi.org/10.1016/j.atmosres.2023.106839>, 2023.
- Yang, F., Tan, J., Zhao, Q., Du, Z., He, K., Ma, Y., Duan, F., Chen, G., and Zhao, Q.: Characteristics of PM_{2.5} speciation in representative megacities and across China, *Atmos. Chem. Phys.*, 11, 5207-5219, <https://doi.org/10.5194/acp-11-5207-2011>, 2011.
- 825 Yang, T., Chen, Y., Zhou, S., Li, H., Wang, F., and Zhu, Y.: Solubilities and deposition fluxes of atmospheric Fe and Cu over the Northwest Pacific and its marginal seas, *Atmos. Environ.*, 239, 117763, <https://doi.org/10.1016/j.atmosenv.2020.117763>, 2020.
- Yang, X., Zheng, M., Liu, Y., Yan, C., Liu, J., Liu, J., and Cheng, Y.: Exploring sources and health risks of metals in Beijing PM_{2.5}: Insights from long-term online measurements. *Sci. Total Environ.*, 814, 151954. <https://doi.org/10.1016/j.scitotenv.2021.151954>, 2022.
- 830 <https://doi.org/10.1016/j.scitotenv.2021.151954>, 2022.
- Yang, Y., Sun, M., Wu, G., Qi, Y., Zhu, W., Zhao, Y., Zhu, Y., Li, W., Zhang, Y., Wang, N., Sheng, L., Wang, W., Yu, X., Yen, P. -H., Yuan, C. -S., Ceng, J. -H., Chiang, K. -C., Tseng, Y. -L., Soong, K. -Y., and Jeng, M. -S.: Inter-comparison of chemical fingerprint and source apportionment of marine fine particles at two islands through the west and east passages of the Taiwan Island. *Sci. Total Environ.*, 851, 158313. <http://dx.doi.org/10.1016/j.scitotenv.2022.158313>, 2022.
- 835 Yen, P. -H., Yuan, C. -S., Wu, C. -H., Yeh, M. -J., Tseng, Y. -L., Soong, K. -Y.: Transport route-based cluster analysis of chemical fingerprints and source origins of marine fine particles (PM_{2.5}) in South China Sea. *Sci. Total Environ.*, 806, 150591. <https://doi.org/10.1016/j.scitotenv.2021.150591>, 2022.
- Yoon, J. E., Yoo, K. C., Macdonald, A. M., Yoon, H. I., Park, K. T., Yang, E. J., Kim, H. C., Lee, J. I., Lee, M. K., Jung, J., Park, J., Lee, J., Kim, S., Kim, S. S., Kim, K., and Kim, I.: Reviews and syntheses: Ocean iron fertilization experiments - past, present, and future looking to a future Korean Iron Fertilization Experiment in the Southern Ocean (KIFES) project, *Biogeosciences*, 15, 5847-5889, <https://doi.org/10.5194/bg-15-5847-2018>, 2018.
- 840 Yu, G., Zhang, Y., Yang, F., He, B., Zhang, C., Zou, Z., Yang, X., Li, N., and Chen, J.: Dynamic Ni/V Ratio in the Ship-Emitted Particles Driven by Multiphase Fuel Oil Regulations in Coastal China, *Environ. Sci. Technol.*, 55, 15031-15039, <https://doi.org/10.1021/acs.est.1c02612>, 2021.
- 845 Yu, J. Z., Huang, X. F., Xu, J. H., and Hu, M.: When aerosol sulfate goes up, so does oxalate: Implication for the formation mechanisms of oxalate, *Environ. Sci. Technol.*, 39, 128-133, <https://doi.org/10.1021/es049559f>, 2005.
- Yu, J., Yao, X., and Zhou, Y.: Characteristics of aerosol aminiums over a coastal city in North China: Insights from the divergent impacts of marine and terrestrial influences. *Sci. Total Environ.*, 918, 170672. <https://doi.org/10.1016/j.scitotenv.2024.170672>, 2024.

- 850 Yuan, C. -S., Hung, C. -M., Hung, K. -N., Yang, Z. -M., Cheng, P. -H., and Soong, K. -Y.: Route-based chemical significance and source origin of marine PM_{2.5} at three remote islands in East Asia: Spatiotemporal variation and long-range transport. *Atmos. Pollut. Res.*, 14, 101762. <https://doi.org/10.1016/j.apr.2023.101762>, 2023.
- Zhang, D., Iwasaka, Y., Shi, G., Zhang, J., Matsuki, A., and Trochkin, D.: Mixture state and size of Asian dust particles collected at southwestern Japan in spring 2000, *J. Geophys. Res.-Atmos.*, 108(D24), 4760, 855 <https://doi.org/10.1029/2003JD003869>, 2003.
- Zhang, D., Iwasaka, Y., Matsuki, A., Ueno, K., and Matsuzaki, T.: Coarse and accumulation mode particles associated with Asian dust in southwestern Japan, *Atmos. Environ.*, 40, 1205–1215, <https://doi.org/10.1016/j.atmosenv.2005.10.037>, 2006.
- Zhang, G., Lin, Q., Peng, L., Yang, Y., Jiang, F., Liu, F., Song, W., Chen, D., Cai, Z., Bi, X., Miller, M., Tang, M., Huang, W., Wang, X., Peng, P. a., and Sheng, G.: Oxalate Formation Enhanced by Fe-Containing Particles and Environmental 860 Implications, *Environ. Sci. Technol.*, 53, 1269-1277, <https://doi.org/10.1021/acs.est.8b05280>, 2019.
- Zhang, H., Li, R., Dong, S., Wang, F., Zhu, Y., Meng, H., Huang, C., Ren, Y., Wang, X., Hu, X., Li, T., Peng, C., Zhang, G., Xue, L., Wang, X., and Tang, M.: Abundance and Fractional Solubility of Aerosol Iron During Winter at a Coastal City in Northern China: Similarities and Contrasts Between Fine and Coarse Particles, *J. Geophys. Res.-Atmos.*, 127, <https://doi.org/10.1029/2021JD036070>, 2022.
- 865 Zhang, J., Zhou, X., Wang, Z., Yang, L., Wang, J., and Wang, W.: Trace elements in PM_{2.5} in Shandong Province: Source identification and health risk assessment, *Sci. Total. Environ.*, 621, 558-577, <https://doi.org/10.1016/j.scitotenv.2017.11.292>, 2018.
- Zhang, L., Gao, Y., Wu, S., Zhang, S., Smith, K. R., Yao, X., and Gao, H.: Global impact of atmospheric arsenic on health risk: 2005 to 2015, *P. Natl. Acad. Sci. USA*, 117, 13975-13982, <https://doi.org/10.1073/pnas.2002580117>, 2020.
- 870 Zhang, Q., Jimenez, J. L., Canagaratna, M. R., Ulbrich, I. M., Ng, N. L., Worsnop, D. R., and Sun, Y.: Understanding atmospheric organic aerosols via factor analysis of aerosol mass spectrometry: a review, *Anal. Bioanal. Chem.*, 401, 3045-3067, <https://doi.org/10.1007/s00216-011-5355-y>, 2011.
- Zhang, T. L., Liu, J. Y., Xiang, Y. X., Liu, X. M., Zhang, J., Zhang, L., Ying, Q., Wang, Y. T., Wang, Y. N., Chen, S. L., Chai, F., and Zheng, M.: Quantifying anthropogenic emission of iron in marine aerosol in the Northwest Pacific with shipborne 875 online measurements. *Sci. Total Environ.*, 912, Article 169158. <https://doi.org/10.1016/j.scitotenv.2023.169158>, 2024.
- Zhang, W., Peng, X., Bi, X., Cheng, Y., Liang, D., Wu, J., Tian, Y., Zhang, Y., and Feng, Y.: Source apportionment of PM_{2.5} using online and offline measurements of chemical components in Tianjin, China. *Atmos. Environ.*, 244, 117942. <https://doi.org/10.1016/j.atmosenv.2020.117942>, 2021.
- Zhang, Y., Cai, J., Wang, S., He, K., and Zheng, M.: Review of receptor-based source apportionment research of fine 880 particulate matter and its challenges in China, *Sci. Total. Environ.*, 586, 917-929, <https://doi.org/10.1016/j.scitotenv.2017.02.071>, 2017.

- Zhang, Y., Deng, F., Man, H., Fu, M., Lv, Z., Xiao, Q., Jin, X., Liu, S., He, K., and Liu, H.: Compliance and port air quality features with respect to ship fuel switching regulation: a field observation campaign, SEISO-Bohai, *Atmos. Chem. Phys.*, 19, 4899-4916, <https://doi.org/10.5194/acp-19-4899-2019>, 2019.
- 885 Zhang, Y., Schauer, J. J., Zhang, Y., Zeng, L., Wei, Y., Liu, Y., and Shao, M.: Characteristics of particulate carbon emissions from real-world Chinese coal combustion, *Environ. Sci. Technol.*, 42, 5068-5073, <https://doi.org/10.1021/es7022576>, 2008.
- Zhao, M., Zhang, Y., Ma, W., Fu, Q., Yang, X., Li, C., Zhou, B., Yu, Q., and Chen, L.: Characteristics and ship traffic source identification of air pollutants in China's largest port, *Atmos. Environ.*, 64, 277-286, <https://doi.org/10.1016/j.atmosenv.2012.10.007>, 2013.
- 890 Zhao, R., Han, B., Lu, B., Zhang, N., Zhu, L., and Bai, Z.: Element composition and source apportionment of atmospheric aerosols over the China Sea. *Atmos. Pollut. Res.*, 6, 191-201. <http://doi.org/10.5094/APR.2015.023>, 2015.
- Zhou, Y., Huang, X. H., Bian, Q., Griffith, S. M., Louie, P. K. K., and Yu, J. Z.: Sources and atmospheric processes impacting oxalate at a suburban coastal site in Hong Kong: Insights inferred from 1 year hourly measurements, *J. Geophys. Res.-Atmos.*, 120, 9772-9788, <https://doi.org/10.1002/2015JD023531>, 2015.
- 895 Zhou, Y.: Elevated Anthropogenic Contributions to Trace Elements in Marine Aerosols Compared to Coastal Qingdao in Eastern China. Figshare [Dataset]. <https://doi.org/10.6084/m9.figshare.29625746>, 2025.
- Zhu, W., Qi, Y., Tao, H., Zhang, H., Li, W., Qu, W., Shi, J., Liu, Y., Sheng, L., Wang, W., Wu, G., Zhao, Y., Zhang, Y., Yao, X., Wang, X., Yi, L., Ma, Y., and Zhou, Y.: Investigation of a haze-to-dust and dust swing process at a coastal city in northern China part I: Chemical composition and contributions of anthropogenic and natural sources, *Sci. Total. Environ.*, 851, 158270, <https://doi.org/10.1016/j.scitotenv.2022.158270>, 2022.
- 900 Zhu, Y., Li, W., Wang, Y., Zhang, J., Liu, L., Xu, L., Xu, J., Shi, J., Shao, L., Fu, P., Zhang, D., and Shi, Z.: Sources and processes of iron aerosols in a megacity in Eastern China, *Atmos. Chem. Phys.*, 22, 2191-2202. <https://doi.org/10.5194/acp-22-2191-2022>, 2022.
- Zhuang, G., Yi, Z., Duce, R. A., and Brown, P. R.: Link between iron and sulphur cycles suggested by detection of Fe(n) in
905 remote marine aerosols. *Nature*, 355, 537-539. <https://doi.org/10.1038/355537a0>, 1992